

The transcription factor Shox2 shapes thalamocortical neuron firing and synaptic properties

Diankun Yu¹, Matthieu Maroteaux¹, Yingnan Song², Xiao Han¹, Isabella Febbo¹, Claire Namboodri¹, Cheng Sun², Wenduo Ye², Emily Meyer¹, Stuart Rowe¹, YP Chen², LA Schrader^{1,2}

- 1. Neuroscience Program, Brain Institute, Tulane University**
- 2. Cell and Molecular Biology, Tulane University**

Running Title: Shox2 affects thalamocortical neuron function

Abstract: 260

Intro: 807

Results: 3063

Discussion: 905

Methods: 3003

Address for LAS:

Cell and Molecular Biology

2000 Percival Stern Hall

6400 Freret St.

New Orleans, LA 70118

schrader@tulane.edu

ABSTRACT

Thalamocortical neurons (TCNs) transmit information about sensory stimuli from the thalamus to the cortex. In response to different physiological states and demands TCNs can fire in tonic and/or phasic burst modes. These firing properties of TCNs are supported by precisely timed inhibitory synaptic inputs from the thalamic reticular nucleus and intrinsic currents, including T-type Ca^{2+} and HCN currents. These intrinsic currents are mediated by Cav3.1 and HCN channel subunits, and alterations in expression or modulation of these channels can have dramatic implications on thalamus function. The factors that regulate these currents controlling the firing patterns important for integration of the sensory stimuli and the consequences resulting from the disruption of these firing patterns are not well understood. *Shox2* is a transcription factor known to be important for pacemaker activity in the heart. We show here that *Shox2* is also expressed in adult mouse thalamus. We hypothesized that genes regulated by *Shox2*'s transcriptional activity may be important for physiological properties of TCNs. In this study, we used RNA sequencing on control and *Shox2* knockout mice to determine *Shox2*-affected genes and revealed a network of ion channel genes important for neuronal firing properties. Quantitative PCR confirmed that expression of *Hcn2*, *4* and *Cav3.1* genes were affected by *Shox2* KO. Western blotting showed expression of the proteins for these channels was decreased in the thalamus, and electrophysiological recordings showed that *Shox2* KO impacted the firing and synaptic properties of TCNs. Finally, behavioral studies revealed that *Shox2* expression in TCNs play a role in somatosensory function and object recognition memory. Overall, these results reveal *Shox2* as a transcription factor important for TCN firing properties and thalamic function.

1 INTRODUCTION

2 Processing of sensory information is mediated by precise circuitry that senses stimuli in
3 the periphery and transforms the information through a network of synaptic connections to
4 ultimately allow perception and cognitive processing of the surrounding world. Rhythmic
5 oscillations of brain activity crucial to cognitive function emerge from neuronal network
6 interactions that consist of reciprocal connections between the thalamus, the inhibitory
7 thalamic reticular nucleus and the cortex¹. Dysfunction of these oscillations caused by
8 aberrant activity in the thalamic circuit is thought to play a role in many neuropathological
9 conditions, including epilepsy²⁻⁴, autism⁵⁻⁷, and schizophrenia⁸⁻¹¹. Furthermore, damage to
10 thalamic nuclei, especially medial and anterior nuclei, causes severe memory deficits known
11 as diencephalic amnesia¹²⁻¹⁷.

12 The intrinsic properties that shape action potential firing and contribute to rhythmic
13 oscillations of the thalamocortical neurons (TCNs) are important for efficient transfer of
14 information from the thalamus to the cortex. Notably, TCNs switch their firing states between
15 2 modes, burst and tonic firing modes that occur at different membrane potentials¹⁸⁻²⁰. The
16 transitions between tonic and burst modes are controlled by several intrinsic conductances
17 within the TCNs, mainly T-type Ca^{2+} currents (I_T) and H-currents (I_h), mediated by Cav3.x and
18 HCN family of channels, respectively¹. Interplay of the kinetics of these currents and other
19 conductances, including leak K^+ , inwardly rectifying K^+ , a persistent Na current and transient
20 A-type currents, can establish a cycle of oscillatory activity that generates rhythmic activity in
21 the thalamocortical network²¹. Consequently, modulation of the intrinsic properties of TCNs
22 is an important regulatory mechanism of firing activity crucial for sensory perception, sleep

23 activity and cognition. Very little is understood about the factors that contribute to
24 modulation of the ion channels that underlie these currents.

25 The transcription factor, *Shox2*, represents a possible mechanism to coordinate
26 expression of ion channels important for TCN firing properties. *Shox2* is a member of the
27 homeobox family of transcription factors²²⁻²⁴, and recent studies suggest it is important for
28 development and maintenance of rhythmic activity in adult heart. Cells in the sinoatrial node
29 of the heart generate spontaneous, rhythmic action potentials and lead other working
30 myocytes to beat at a stable firing rate, thus these cells are known as pacemaker cells²⁵. The
31 rhythmic action potential generation in the pacemaker cells is mediated by the prominent
32 expression of HCN channels and T-type calcium channels^{26,27}. We and others have shown that
33 *Shox2* plays a decisive role in the differentiation of pacemaker cells in the sinoatrial node of
34 the heart and pulmonary vein in mice, and *Shox2* expression in the SAN is necessary for
35 cardiac pacemaker-type activity^{28,29}. Importantly, *Shox2* is essential for expression of HCN4
36 channels²⁸, and *Shox2* overexpression favors differentiation of mouse embryonic stem cells
37 into pacemaker cells with biological pacing ability and enhanced HCN currents³⁰. *Shox2*
38 expression in the sinoatrial node of the heart continues into adulthood since cells of the
39 sinoatrial node maintain pacemaker properties, while *Shox2* expression is suppressed in
40 pulmonary vein and coronary sinus in the adult, and these cells lose pacemaker properties
41 during development³¹. These results suggest that *Shox2* expression is critical for expression of
42 channels important for myocyte firing properties and is a determinant of pacemaker
43 properties of the sinoatrial node.

44 During development of the nervous system, *Shox2* expression has been reported in
45 neurons of the facial motor nucleus (nVII)³², cerebellum³³, spinal cord³⁴ and dorsal root
46 ganglia³⁵. *Shox2*-expressing excitatory interneurons in the ventral spinal cord are rhythmically

47 active during locomotor-like activity, and synaptic and electrical connections between *Shox2*-
48 expressing interneurons are crucial for the frequency and stability of their rhythmic activity³⁴,
49 ³⁶, showing that interconnectivity between *Shox2*-expressing neurons is critical for
50 synchronization of rhythmic activity. These results suggest that *Shox2*-expressing neurons play
51 a critical role in central pattern generation important for locomotion, but the role of *Shox2* in
52 this rhythmic behavior was not further investigated.

53 In this study, we found that *Shox2* is expressed in thalamocortical neurons (TCNs) in adult
54 mice. TCNs express HCN2, HCN4 and Ca_v3.1 channel protein subunits that are important for
55 firing properties of TCNs, and we hypothesized that *Shox2* coordinates the expression of genes
56 for these ion channels to affect action potential firing activity of TCNs. Using conditional KO
57 animals, we further demonstrated that *Shox2* is important for tonic spike frequency firing
58 properties in TCNs, likely by affecting expression multiple ion channels, including HCN. We
59 also demonstrated that an inducible global knock-out of *Shox2* reduced anxiety behavior in
60 the open field, impaired sensorimotor function and object recognition memory. Object
61 recognition memory deficits were confirmed with an inducible *Shox2* knock-out in medial
62 thalamus. The present study provides novel insight into the molecular markers that contribute
63 to thalamocortical neuron function and shows that *Shox2* expression is critical to maintain
64 thalamic neuron function and physiological properties by regulating gene expression in the
65 neurons of the adult mouse thalamus.

66

67 **Methods**

68 **Mice**

69 All animal procedures were approved by Tulane University Institutional Animal Care and
70 Use Committee (IACUC) according to National Institutes of Health (NIH) guidelines. *Shox2*
71 transgenic mice including *Shox2^{Cre}*, *Shox2^{LacZ}*, *Shox2^{ff/ff}* and *Rosa26^{CreERT}* mice were generously
72 donated by Dr. Yiping Chen. All wildtype C57Bl/6N mice were ordered from Charles River.
73 *Rosa26^{LacZ/+}* (stock #003474) and *Gbx2^{CreERT/+}* breeders (stock #022135) were ordered from
74 Jackson Lab.

75 In inducible KO experiments, *Rosa26^{CreERT/+}*, *Shox2^{ff/ff}* or *Rosa26^{CreERT/CreERT}*, *Shox2^{ff/ff}* female
76 mice were crossed with *Shox2^{-/+}* male mice or, in the case of the *Gbx2* animals,
77 *Gbx2^{CreERT/+}*, *Shox^{ff/ff}* or *Gbx2^{CreERT/CreERT}*, *Shox^{ff/ff}* were crossed with *Shox2^{-/+}* male mice
78 (Supplemental Fig. 1). Litters were labelled and genotyped at postnatal day 10 (P10). The KO
79 group was the *Rosa26^{CreERT/+}*, *Shox2^{-/ff}* mice (*Gbx2^{CreERT/+}*, *Shox2^{-/ff}*) and the control (CR) group
80 was the littermate *Rosa26^{CreERT/+}* (*Gbx2^{CreERT/+}*), *Shox2^{+/ff}*. In the *Shox2^{LacZ/+}* and *Shox2^{Cre/+}* mice,
81 the first two exons of the *Shox2* allele were partially replaced by *LacZ* and *Cre* genes
82 respectively in order to obtain the expression of *LacZ* mRNA and *Cre* mRNA under the control
83 of the *Shox2* promoter, while the unaffected alleles express *Shox2* mRNA²⁴. The *Rosa26^{CreERT/+}*
84 mouse line is a transgenic mouse line with a tamoxifen-inducible Cre^{ERT} inserted in the *Rosa26*
85 loci. The *Rosa26^{LacZ/+}* mouse line is a transgenic mouse line with a floxed stop signals followed
86 by *LacZ* gene inserted in the *Rosa26* loci³⁷. This ‘cre reporter’ mouse strain was used to test
87 the expression of the *Cre* transgene under the regulation of a specific promoter.

88 The *Rosa26^{CreERT}* is a global KO, whereas the *Gbx2^{CreERT}* mouse was used to knockdown
89 *Shox2* specifically in the medial thalamus. Our localization studies with *Gbx2*-promotor driven
90 GFP staining showed that *Gbx2* promotor-driven *CreERT* is specifically expressed in the medial

91 thalamus of the $Gbx2^{CreErt}$ adult mouse (Supplemental Fig. 2A). Further testing using RT-qPCR
92 showed that *Shox2* mRNA was reduced in the medial thalamus of the $Gbx2^{CreRt/+}$, $Shox2^{-/f}$
93 compared to CR mice, but not lateral thalamus (Supplemental Fig. 2B).

94 To induce recombination in animals bearing a Cre^{ERT2} , pre-warmed tamoxifen (100-160
95 mg/kg) was injected intraperitoneally into KO mice and CR littermates at the same time every
96 day for five consecutive days. Tamoxifen (20 mg/mL) was dissolved in sterile corn oil (Sigma,
97 C8267) with 10% alcohol. The littermate KO mice and CR mice of the same sex were housed
98 together and received the same handling. Throughout experiments, the researchers were
99 blinded to the genotype. RT-qPCR experiments were used to confirm the efficiency of *Shox2*
100 KO in brains in every animal tested.

101 In order to view projections of *Shox2*-expressing neurons, we created the *Ai27D-Shox2Cre*
102 mouse. B6.Cg-Gt(ROSA)26Sortm27.1(CAG-COP4*H134R/tdTomato)Hze/J(Ai27D) mice from
103 Jackson labs were crossed with *Shox2Cre* to obtain mice with *Shox2*-expressing neurons
104 labeled with tdTomato and expressing Chr2 (figure 2 M-O).

105 **X-gal staining**

106 Adult $Shox2^{LacZ/+}$ or $Shox2^{Cre/+}$, $Rosa26^{LacZ/+}$ male mice were anaesthetized by isoflurane
107 inhalation, decapitated, and the brains were removed. Brains were sliced at 200 μ m using a
108 Vibratome Series 3000 Plus Tissue Sectioning system. Brain slices were placed into ice-cold
109 artificial cerebrospinal fluid (aCSF) in a 24-well plate and fixed with 0.5% glutaraldehyde and
110 4% paraformaldehyde in phosphate buffered saline (PBS) for 15 minutes. After 3X wash with
111 ice-cold PBS, the slices were incubated with X-gal staining solution, containing: (X-gal (1mg/ml),
112 potassium ferrocyanide (4 mM), potassium ferricyanide (4mM) and $MgCl_2$ (2 mM) and covered
113 by aluminum foil at 37 °C overnight. All slices were washed and post-fixed. Images were taken
114 under a stereo microscope.

115 **Immunohistochemistry (IHC)**

116 Mice were deeply anaesthetized by injection with ketamine (80 mg/kg) mixed with
117 xylazine (10 mg/kg), perfused transcardially with ice-cold phosphate-buffered saline (PBS)
118 followed by 4% paraformaldehyde in PBS and decapitated for brain collection. Mouse brains
119 were placed in 4% paraformaldehyde in PBS at 4° C overnight for post-fixation. In order to
120 perform cryostat sections, the brains were sequentially placed in 15% and 30% sucrose in PBS
121 solutions at 4 °C until saturation. The brain samples were embedded with optimal cutting
122 temperature compound (OCT) and stored at -20 °C and cryo-sectioned in 20-50 µm coronal
123 slices with Leica CM3050S cryostat. For IF staining, slices were washed with 50 mM Tris
124 Buffered Saline with 0.025% Triton X-100 (TTBS) and blocked in 2% Bovine Serum Albumin
125 (BSA) in TTBS for 2 hours at room temperature. Primary antibodies were diluted in blocking
126 solutions and applied on slides overnight at 4°C. Fluorescence-conjugated secondary
127 antibodies were diluted 1:1000 in blocking solutions and applied on slides for one hour at
128 room temperature. 1:1000 DAPI was applied for 5 minutes at room temperature for nuclei
129 staining and washed. The slices were mounted on slides with mounting media (Vector
130 Laboratories, H-1000) and imaged under confocal microscope.

131 **mRNA Sequencing**

132 Thalamus mRNA was extracted from 3 KO mice and 3 CR mice and sent to *BGI Americas*
133 *Corporation (Cambridge, MA, USA)* for RNA-seq quantification. Total RNA was isolated in
134 tissue from the midline of the thalamus of P60 male *Gbx2^{CreERT/+}, Shox2^{-/f}* mice and control
135 male littermates (*Gbx2^{CreERT/+}, Shox2^{+/f}*) with the same method used for RT-qPCR RNA
136 extraction. Around 30 million single-end 50-bp reads by BGISEQ-500 Sequencing Platform per
137 sample were aligned to the mm10/GRCm38 mouse reference genome using Salmon v0.10.2
138 ³⁸. The count data from Salmon v0.10.2 was analyzed via DESeq2 v 1.22.2 ³⁹ to identify genes

139 differently expressed (DEGs) between KO and CR and to calculate Fragments Per Kilobase
140 Million (FPKMs). Genes with adjusted p value < 0.1 were defined as DEGs and were used for
141 further gene ontology (GO) analysis through online DAVID Bioinformatics Resources ^{40, 41}.

142 **Quantitative reverse transcription PCR (RT-qPCR)**

143 The whole thalamus was collected from adult mouse brains (*Rosa^{CreErt}-Shox2* KO) and
144 immediately stored in RNAlater™ RNA stabilization reagent (ThermoFisher Scientific,
145 AM7021). RNA was extracted using RNeasy Mini Kit (Qiagen, 74104) following the standard
146 protocol provided in the manual. The RNA concentration and quality were tested using
147 Nanodrop Microvolume Spectrophotometers and Fluorometer as well as agarose gel
148 investigation. Reverse transcription was conducted using iScript™ Reverse Transcription
149 Supermix (Bio- Rad, 1708840). Quantitative PCR was conducted with iTaq™ Universal SYBR
150 Green Supermix (Bio-rad, 1725121) in Bio-Rad CFX96 Touch™ PCR system. Data analysis was
151 done with CFX Manager software. The expression of all the genes tested in the RT-qPCR
152 experiments were normalized to the widely used housekeeping reference gene β -actin (*Actb*)
153 and TATA-box binding protein (*Tbp*) ^{42, 43}. All primers were designed and tested, and conditions
154 were optimized to have an efficiency between 95% and 105%. Both the melt curves and gel
155 investigations were used to confirm the RT-qPCR products. The primer sequences of all tested
156 genes including reference gene *Actb* and *Tbp* are listed in Table 1.

157 To confirm knock-down of *Shox2* in the *Gbx2^{CreERT/+}* animals, adult *Gbx2^{CreERT/+}; Shox2^{-f}*
158 male and female mice were anaesthetized by isoflurane inhalation followed decapitation. The
159 brains were removed and a 1 mm thick slice through the thalamus was removed via razor
160 blade, the location of cut is determined by Paxinos and Franklin Mouse Brain Atlas. Medial
161 thalamus tissue is collected with 1mm stainless steel punching tool and lateral thalamus was
162 separated via razor blade. The collected tissues were stored in 50 μ L RNA later solution and

163 stored in -80 freezer. To homogenize collected tissues, 350 μ L of RLT lysis buffer from Qiagen
164 RNeasy Mini Kit is added to the tissue and homogenized with a pestle mortar. The
165 homogenized tissues went through sonication with a Q55 sonicator (Qsonica) and then 350
166 μ L cold, 70% EtoH was added to the sample. After this, the mixed solution is processed by
167 series of spin and wash follow the instructions book from Qiagen RNeasy Mini Kit. Once RNAs
168 are isolated from tissues, we applied qRT-PCR with Shox2 primer (Table 1) and normalized
169 with GAPDH.

170
171
172

Table 1. Sequences of RT-qPCR primers

Gene	Forward Primer(5'->3')	Reverse Primer (5'->3')
<i>Shox2</i>	CCGAGTACAGGTTTGGTTTC	GGCATCCTTAAAGCACCTAC
<i>actb</i>	CTAGACTTCGAGCAGGAGAT	GATGCCACAGGATTCCATAC
<i>Tbp</i>	CCGTGAATCTTGGCTGTAACTTG	GTTGTCCGTGGCTCTCTTATTCTC
<i>Hcn1</i>	CTTCGTATCGTGAGGTTTAC	GTCATAGGTCATGTGGAATATC
<i>Hcn2</i>	CTTTGAGACTGTGGCTATTG	GCATTCTCCTGGTTGTTG
<i>Hcn4</i>	ATACTTATTGCCGCCTCTAC	TGGAGTTCTTCTTGCCTATG
<i>Cacna1g</i>	GACACCAGGAACATCACTAAC	CACAAACAGGGACATCAGAG
<i>Cacna1h</i>	TTTGGGAATATGTGCTCTTC	TCTAGGTGGGTAGATGTCTTATC
<i>Gapdh</i>	GTCGGTGTGAACGGATTTG	TAGACTCCACGACATACTCAGCA.

173

174 **Western Blot**

175 Thalamic tissues were collected from the adult mouse brains and immediately placed
176 on dry ice and stored at -80 °C until use. The thalamus samples were lysed with RIPA lysis
177 buffer (150 mM Sodium chloride, 1% Triton X-100, 0.5% sodium deoxycholate, 0.1% SDS, 50

178 mM Tris, pH 8.0) with fresh added Halt™ protease inhibitor cocktail (ThermoFisher Scientific,
179 78430). Samples were centrifuged at 12,000 rpm at 4 °C for 20 minutes and the supernatant
180 protein samples were collected. The protein concentration of the samples was determined
181 using the Bio-Rad DC protein assay (Bio-Rad, 500-0116). Samples were normalized with the
182 same lysis buffer, aliquoted and stored at -80°C until use. Before loading, 5X sample buffer
183 (ThermoFisher Scientific, 39001) and dithiothreitol (final concentration - 50 mM, DTT) were
184 added to each protein sample. Sample mixtures were left at room temperature for 30 minutes.
185 Protein (20-30 µg/well) was loaded in a SDS-PAGE gel (4% stacking gel and 8% separating gel),
186 together with 3 µL prestained protein ladder (ThermoFisher Scientific, 26619). The gels were
187 run at 70 mV for 3 hours, and the proteins were transferred to a pre-activated PVDF
188 membrane (Millipore, IPFL00005) at -70 mV for 3 to 4 hours. Sodium dodecyl sulfate (SDS)
189 and methanol were added into transfer buffer at a final concentration of 0.1% and 10%,
190 respectively. The gels were stained with Coomassie Brilliant Blue solution (0.1% Coomassie
191 Brilliant Blue, 50% methanol, 10% Glacial acetic acid) to check that no obvious proteins
192 remained under these transfer conditions. Membranes were incubated in blocking solution
193 with 5% non-fat dry milk and 3% BSA in TTBS at room temperature for one hour. Primary
194 antibody was diluted in Odyssey^R Blocking Buffer in TBS and applied on the membrane at 4 °C
195 overnight. After washing the membrane with TTBS, fluorescence-conjugated secondary
196 antibodies were diluted and applied on the membrane at room temperature for one hour.
197 Imaging of the stained membrane was done in an Odyssey CLx Infrared Scanner and analyzed
198 by Image Studio Lite Ver 5.2.

199

200

201

202 **Antibodies used in IHC and Western blot experiment**

Reagent/Resource	Supplier	Details
Chicken anti- β -galactosidase	Abcam	Ab9361; 1:500
Rabbit anti-NeuN Cy3- conjugated	Millipore Sigma	ABN78; 1:500
Mouse anti-parvalbumin	Millipore Sigma	MAB1572; 1:500
Rabbit-anti GFAP	PhosphoSolutions	620-GFAP; 1:300
Rabbit-anti GFP	Novus Biologicals	NB 600-308; 1:300
Alexa-Fluor 488 Goat anti-mouse	Life Technologies	1:1000
Alexa-Fluor 647 Goat anti-chicken	Life Technologies	1:1000
Alexa-Fluor 594 Goat anti-rabbit	Life Technologies	1:1000
mouse anti-HCN2	Neuromab	N71/37; 1:1000
mouse anti-HCN4	Neuromab	N114/10; 1:1000
mouse anti-Cav3.1	Neuromab	N178A/9; 1:1000
IRDye 680RD Goat anti-mouse	Li-Cor	P/N 926-68070; 1:10,000
IRDye 800CW Goat anti-rabbit IgG (H+L)	Li-Cor	P/N 926-32211; 1:10,000

203

204 **Electrophysiology**

205 At the same time of the day (11:00 am summer and 10:00 am winter), male and female
206 mice (PND 60-120) were anaesthetized with isoflurane and decapitated. Brains were quickly
207 removed and immersed in oxygenated (95% O₂ and 5% CO₂), ice-cold N-methyl-D-glucamine
208 (NMDG)-based slicing solution (in mM, 110 NMDG, 110 HCl, 3 KCl, 1.1 NaH₂PO₄, 25 NaHCO₃,
209 25 Glucose, 10 ascorbic acid, 3 pyruvic acid, 10 MgSO₄, 0.5 CaCl₂). The first 350 μ m coronal
210 brain section containing the most anterior paraventricular thalamus (PVA) was obtained with
211 a Vibratome Series 3000 Plus Tissue Sectioning System. The collected brain slices were
212 transferred and incubated in oxygenated standard aCSF (in mM, 125 NaCl, 2.5 KCl, 26 NaHCO₃,

213 1.24 NaH₂PO₄, 25 Dextrose, 2 MgSO₄, 2 CaCl₂) at 37 °C for 30 minutes, then incubated at room
214 temperature until use.

215 During the recordings, an individual slice was transferred to a recording chamber and
216 perfused with oxygenated external solution at a speed of 1 mL/minute at room temperature
217 at room temperature. Unless otherwise specified, standard aCSF was perfused as the external
218 solution. For isolation of the specific currents, different pharmacological antagonists were
219 applied in the external solution as stated in the results. PVA was identified as the nucleus near
220 the border of the third ventricle enclosed by the stria medullaris. Cell-attached and whole-cell
221 recordings were obtained using MultiClamp 700B amplifier, Digidata 1322A digitizer, and a PC
222 running Clampex 10.3 software (Molecular Device). For cell-attached recording, glass pipettes
223 had resistances of 2.5 – 3.5 MΩ filled with standard aCSF. Giga seals were obtained in every
224 cell by application of a small negative pressure for spontaneous action potential recording.
225 For intracellular whole-cell patch clamp recording, glass pipettes had resistances of 3.5 – 6
226 MΩ filled with internal pipette solution (in mM, 120 Kgluconate, 20 KCl, 0.2 EGTA, 10 Hepes,
227 4 NaCl, 4 Mg²⁺ATP, 14 phosphocreatine, 0.3 Tris GTP (pH was adjusted to 7.2-7.25 by KOH,
228 osmolarity was adjusted to 305-315 mOsm by sorbitol). Series resistance was monitored and
229 only cells with series resistance less than 20 MΩ and that did not change over 15% throughout
230 the recording were further analyzed. Spontaneous action potentials were recorded in current
231 clamp mode at membrane potential. Cells with no action potentials identified in 5 minutes
232 are classified as 'not active' cells. Action potential threshold was measured on the first spike
233 at the point where the voltage change reaches 20 mV/ms.

234 HCN currents were isolated under voltage-clamp. The external solution for HCN current
235 isolation contained 0.5 μM TTX, 1 mM NiCl₂, 1 mM CdCl₂, 2 mM BaCl₂, 10 μM DNQX and APV
236 to block voltage-gated sodium channels, voltage-gated calcium channels, inwardly-rectifying

237 potassium channels and excitatory synaptic current respectively. NaH_2PO_4 was omitted to
238 prevent precipitation with cations.

239 **Behavioral assays**

240 If a timeline is needed, P21-P25 tamoxifen injection; ~around P56 1-2 weeks handling; then 3
241 day habituation of the room, 1 day open field, 2 days NOR, 1 weeks later paw sensation, 1
242 weeks later forced swim, at least 1 weeks later tail suspension. 3 days handling before each
243 test.

244 An open field test was used to test mouse exploratory behavior and anxiety-related
245 behavior. The experiments were all done 2 hours into the animal's dark light phase under dim
246 red light. All mice received routine handling for a week. Three days before the experiments,
247 mice were habituated to the training and testing room for 1 hour each day. On the first day of
248 experiments, each mouse was placed in the open field (16 inches x 16 inches) and allowed to
249 explore freely under dim red light for 5 minutes. Infrared beams and computer-based software
250 *Fusion* were used to track mice and calculate mice activity and time spent in the center (8
251 inches x 8 inches) of total open field.

252 In novel object recognition (NOR) experiments, all mice received routine handling and
253 three days habituation to the experimental room before the experiments. On the day before
254 the familiarization trial, each mouse was placed in the open field in the absence of objects
255 and allowed to explore it freely, the behaviors were recorded and analyzed further as open
256 field test data. In the familiarization trial, each mouse was placed in the open field containing
257 two identical 100 ml beakers in the neighboring corners for 5 minutes. Twenty-four hours later,
258 each mouse was placed back in the same open field with two objects, one of which was the
259 100 ml beaker and the other one a padlock of a similar dimension, for a 5-minute testing trial.
260 To prevent bias in objects exploration, mice were always released on the opposite side from

261 the object for both familiarization and testing trials. For NOR and the subsequent behavior
262 experiments, mouse behaviors in the testing trials were video-taped and analyzed by
263 experimenters who were blind to the genotypes of the mice. Exploration of an object was
264 defined as sniffing and touching the object with attention, whereas other behaviors like
265 running around the object, sitting or climbing on it were not recorded as exploration ⁴⁸.
266 Discrimination index was calculated as $(t_n - t_f)/(t_n + t_f)$. Where t_n = time exploring new object
267 and t_f = time exploring familiar object. In the *Gbx2Cre,Shox2* KO test, 2 animals exhibited a
268 preference for one object in the familiarization trial and therefore were not tested the next
269 day.

270 The adhesive removal test was used to assess mouse paw sensorimotor response ⁴⁹. A
271 small piece of round sticky paper tape (Tough-spots, for microtube cap ID, ~1 cm², Research
272 Products International Corp. 247129Y) was applied to the plantar surface of the right hind paw
273 of each mouse, and the mouse was placed back in its home cage and the behavior recorded.
274 The latency to the first response to the tape was measured and analyzed.

275 The tail suspension test and forced swim test were applied to assess and evaluate
276 mouse depressive-like behaviors ⁵⁰. In the tail suspension test, a 5-cm of the tip of Falcon 15
277 mL conical centrifuge tube was placed around the tails to prevent tail climbing, and each
278 mouse was suspended by the tail for 5 minutes. The behavior of the mice was recorded and
279 analyzed. The escape-related struggling time within the 5-minute experiment was measured
280 as mobility time.

281 In the forced swim test, each mouse was placed in a 1000 ml beaker with ~800 ml water
282 for 5 minutes. The behavior of the mouse was taped and analyzed by experimenters who were
283 blinded to genotypes of the mice. Swimming and intentional movements with all four legs or

284 body were measured as mobility time, and small movements of front or hind legs made by
285 the animal to stay at the surface were not counted as mobility.

286 Fear Conditioning: Fear conditioning (habituation, training and testing) was performed
287 and filmed in standard operant chambers (Med Associates, video fear conditioning). All
288 behaviors were recorded, and mobility or freezing behavior was assessed online by Medical
289 Associates Video Freeze software.

290 The fear conditioning protocol occurred over 4 days as follows:

291 Day 1: Habituation - each animal was placed in the operant chamber for 10 minutes.

292 Day 2: Training - each animal was placed in the chamber for a total of 8 minutes. The
293 training trial was two mild training sessions consisting of a 30 sec auditory cue (administered
294 at 3 and 5 minutes after placement in chamber) that co-terminated with a single 2 second 0.5
295 mA shock. The animal was removed from the chamber after 8 minutes.

296 Day 3: Context Testing: Animal was placed in the chamber for 5 minutes and behaviors
297 recorded.

298 Day 4: Cued testing - the chamber was modified (plastic floor and inserts to allow
299 different shape), and different olfactory cues (vanilla) were given. The cue was administered
300 after 3 minutes chamber exploration and freezing to the cue was assessed as described above.
301 Animals were removed from the chamber after 6 minutes.

302 **Statistics**

303 Unless otherwise noted in the text, control and KO results were compared using a
304 Student's unpaired t-test. In some cases of unequal variance, the Mann Whitney
305 nonparametric test is used instead of t-test.

306

307

308 **Results**

309 ***Shox2* is specifically expressed in the thalamic neurons in the brain of young adult mouse.**

310 To investigate the expression of *Shox2* in postnatal mouse brain, coronal brain slices from
311 P25 and P60 *Shox2^{LacZ/+}* mice were stained with X-gal, in which the expression of *LacZ* indicated
312 *Shox2* expression (Supplemental Fig. 3 A, B). The X-gal staining results indicated that *Shox2* is
313 expressed throughout the dorsal thalamus including medial thalamus, anterior thalamus
314 nuclei (ATN), ventrobasal nucleus (VB), dorsal lateral geniculate nucleus (dLGN), and medial
315 lateral geniculate nucleus (MGN) but not in other regions of diencephalon including habenula,
316 reticular nucleus of the thalamus and hypothalamus, or other regions of the nervous system
317 like the cortex, subcortical regions of the forebrain, hippocampus, amygdala, cerebellum and
318 spinal cord. To determine whether the expression pattern of *Shox2* changes during
319 development, coronal brain slices from a P56 *Shox2^{Cre/+}, Rosa26^{LacZ/+}* mouse in which *LacZ* is
320 expressed in all cells that have expressed *Shox2* at any time during development were stained
321 with X-gal (Supplemental Fig. 3C). These results showed that the expression of *Shox2* is
322 relatively restricted to the dorsal thalamus in the adult as well as during development, with
323 sparse expression extended to habenula and superior and inferior colliculus and nuclei within
324 the brainstem in the developing animal. We further assessed the cell type of *Shox2*-expressing
325 cells.

326 In order to determine the cell types in which *Shox2* is expressed, thalamic neurons were
327 labeled with the neuronal nuclear protein antibody (NeuN) which is specifically expressed in
328 mature neurons^{51, 52}. *Shox2* was co-expressed in most, but not all, NeuN-positive cells
329 throughout the dorsal thalamus from rostral to caudal (Fig. 1 A-C). Importantly, all *Shox2*-
330 labeled cells were NeuN-positive, suggesting that *Shox2* expression is restricted to neurons.
331 To confirm that *Shox2* was not expressed in astrocytes, the co-expression of *Shox2* and Glial

332 Fibrillary Acidic Protein (GFAP), which labels astrocytes^{53, 54} was assessed. GFAP was
333 expressed at relatively low levels in the thalamus but highly expressed in the hippocampus
334 (supplemental Fig. 4), and *Shox2* was not expressed in the GFAP-positive astrocytes
335 throughout the thalamus (Fig. 1D-F). Together these results show that *Shox2* is expressed in
336 neurons and not GFAP-positive astrocytes.

337 To determine if *Shox2* is expressed in GABAergic neurons, immunohistochemistry (IHC)
338 with parvalbumin (PV) on coronal brain sections from *Shox2*^{Cre/+}, *Rosa26*^{LacZ/+} mice was
339 performed (Fig. 2). Parvalbumin (PV) is highly expressed in the interneurons of the reticular
340 nucleus of thalamus, which borders the thalamus laterally and ventrally. PV labeling
341 delineated the reticular nucleus that defined the border of the thalamus. The PV staining
342 results confirmed the results shown in supplemental figure 4 that during development, *Shox2*
343 is expressed throughout the thalamus (Fig. 2) and sparsely in the habenula (Fig. 2D) and
344 midbrain (Fig. 2I). Importantly, *Shox2* was not expressed at any point during development in
345 cells of the cortex (Fig. 2C), reticular nucleus of the thalamus (Fig. 2E, F), hypothalamus (Fig.
346 2G) or hippocampus (Fig. 2I). In addition, our results showed few PV+ cells in the thalamus as
347 previously reported⁵⁵, and *Shox2* was not co-expressed in PV+ cells (Fig. 2G). These results
348 suggest that *Shox2* is not expressed in parvalbumin-expressing inhibitory interneurons.

349 Finally, the expression and projections of *Shox2*-expressing neurons were investigated
350 using *Shox2*^{Cre/+}; *Rosa*^{tdTomato-ChR2} mice. These mice allow labeling of *Shox2*-expressing neurons
351 with td-Tomato and manipulation of *Shox2*-expressing neurons with Channelrhodopsin-2.
352 Interestingly, we found that the *Shox2*-expressing neurons projected to multiple cortical areas,
353 including retrosplenial and somatosensory cortices with a clear delineation of the barrel fields
354 in somatosensory cortex (Fig. 2M-O). Further strong projections from *Shox2*-expressing
355 neurons were observed within the thalamus, particularly the VB complex, in reticular nucleus

356 of thalamus and internal capsule (Fig. 2 M-O) projecting to somatosensory cortex. In summary,
357 the X-gal staining and immunofluorescence results indicated that *Shox2* expression was
358 restricted to excitatory thalamocortical neurons in the adult stage.

359

360 ***Lack of Shox2 affects gene expression in TCNs***

361 To study the specific role of *Shox2* in regulation of gene expression in neurons of adult
362 thalamus, RNA sequencing was performed. For this experiment, the inducible knockout (KO,
363 $n = 3$) of *Shox2* in *Gbx2*^{CreERT/+}, *Shox2*^{-/-} mice were compared to littermate *Gbx2*^{CreERT/+}, *Shox2*^{+/-}
364 control (CR, $n = 3$) mice. Our GFP staining results showed *Gbx2* is specifically expressed in the
365 medial thalamus from P21 (Supplemental fig. 2), so we ran mRNA sequencing with RNA
366 extracted from medial thalamus of the CR and KO mice. Our results showed 372 differentially
367 expressed genes (DEG) between CR and KO mice, 212 of which are downregulated and 160
368 are upregulated in KO tissue (Supplemental file and Fig. 3A). Gene Ontology (GO) analysis
369 showed *Shox2* KO affected genes in GO terms of ion channel activity, learning and locomotory
370 behavior (Fig. 3B). Importantly, *Shox2* KO downregulated the expression of *Hcn2*, *Hcn4* and
371 *Cacna1g* genes (Supplemental file and Fig. 3A). The protein products of these genes, HCN2,
372 HCN4 and Cav3.1 mediate HCN current and T-type Ca²⁺ currents, respectively. Since these
373 channels are significant contributors to the rhythmic firing properties of TCNs, we further
374 pursued mRNA and protein expression of these channels.

375 To confirm *Shox2* regulates ion channel-related genes in the whole thalamus, another
376 transgenic mouse line, the global KO (*Rosa26*^{CreERT/+}, *Shox2*^{-/-} mice), in which *Shox2* was
377 reduced in the whole thalamus was used. The RNA was extracted from KO (*Rosa26*^{CreERT/+},
378 *Shox2*^{-/-} mice) and CR (*Rosa26*^{CreERT/+}, *Shox2*^{f/+}) mice, and RT-qPCR was performed. The Cav3
379 family of Ca²⁺ channel subunits encode I_T and is highly expressed in the nuclei of the thalamus

380 ^{56, 57}. We tested the levels of mRNA expression for Cav3.1 and Cav3.2, which are coded by
381 *Cacna1g* and *Cacna1h*, respectively. Previous studies showed that Cav3.1 protein subunits are
382 the primary T-type calcium channel proteins expressed in the thalamocortical neurons, while
383 Cav3.2 proteins are expressed at lower levels in the thalamus and the prominent subunit in
384 the reticular nucleus of the thalamus ⁵⁸⁻⁶¹. Our results showed that expression of *Cacna1h*
385 expression was very low in the thalamus, which confirmed the specificity of our thalamic
386 dissection (Supplemental Fig. 2C) and there was no significant difference in *Cacna1h*
387 expression between CR and KO (Student's t-test, $t_9=1.02$, $P=0.34$). With respect to the
388 expression of *Cacna1g*, *Shox2* KO significantly decreased the mRNA expression of *Cacna1g*
389 (Fig. 3C; Student's t-test, $t_9=3.85$, $P<0.01$) in the thalamic tissue. These results confirmed the
390 mRNA sequencing data and suggest Cav3.1 channels that contribute to the T-type currents
391 are down-regulated in the thalamus.

392 The mRNA expression of HCN channel genes in CR and KO mice was also assessed.
393 Previous studies reported that mouse brains express very low levels of *Hcn3* ⁶², and our RNA-
394 seq data showed no significant change in *Hcn3* or expression in the KO mice, therefore, *Hcn3*
395 expression was not further investigated. The expression levels of mRNAs for *Hcn1*, *Hcn2*, and
396 *Hcn4* were investigated. Our results show that *Hcn2* mRNA was the most highly expressed
397 HCN channel gene in the thalamus tissue. *Hcn4* also had prominent expression, while the level
398 of expression of *Hcn1* was only about 5% of *Hcn2* expression. This result is consistent with
399 previous research indicating HCN2 and 4 channels are the most highly expressed HCN
400 channels in the thalamus, and these results along with our sequencing results, provide relative
401 expression data of HCN mRNA expression in mouse thalamus ⁶². *Hcn1* mRNA expression levels
402 were not significantly affected by *Shox2* KO in comparison to CR mice ($t_9=1.85$, $P=0.10$). *Hcn2*
403 and *Hcn4* mRNA were significantly reduced in the *Shox2* KO thalamus compared to CR mice

404 (Fig. 3D, E, *Hcn2*: $t_9=3.92$, $P<0.01$ and *Hcn4*: $t_9=4.02$, $P<0.01$: Mann Whitney nonparametric
405 test). This result also confirmed the RNA-seq results that showed that *Hcn1* mRNA was not
406 significantly affected in mouse thalamus. Together, these results show that *Shox2* KO
407 significantly affects expression of mRNAs for HCN and Ca^{2+} channels. We further investigated
408 if the proteins for these channels were also affected in the KO mice.

409 Western blot experiments on whole thalamus extract were performed to test the protein
410 levels of the Cav3.1, HCN2 and HCN4 channels. The expression levels of HCN4 proteins were
411 significantly decreased in the thalami of KO animals, and there was a trend toward decreased
412 expression of HCN2 and Cav3.1 proteins compared to CR mice (Fig. 3F,G,H; Cav3.1: $t_{14}=1.86$,
413 $P=0.08$; HCN2: $t_{16}=2.30$, $P=0.1$; Mann Whitney nonparametric test; HCN4: $t_{14}=2.37$, $P=0.03$).
414 The protein measurements in these Western blot staining results are consistent with
415 sequencing and RT-qPCR results and confirmed that HCN4 protein expression is modulated by
416 *Shox2* in the adult thalamus. While the change in expression of these channels is relatively
417 small, it's important to note that these data are taken from the entire thalamus, including
418 neurons and glial cells that do not express *Shox2*. The consistency of the sequencing, mRNA
419 and protein expression is solid evidence that *Shox2* affects expression of these ion channel
420 genes.

421 Since the expression levels of the channel proteins that underlie currents important for
422 the bursting properties of the thalamic neurons are regulated by *Shox2* expression, we
423 assessed the firing and intrinsic properties of thalamic neurons in *Shox2* KO and CR mice. To
424 best identify a single thalamic nucleus and a homogenous neuron group, the anterior
425 paraventricular thalamus (PVA), the most rostral and dorsal midline nucleus, was chosen as
426 the target region for recording. First, cell-attached voltage-clamp recordings were performed
427 to record the spontaneous action potential currents of PVA neurons without rupturing the cell

428 membrane. Our results indicated that a smaller percentage of cells fired spontaneous action
429 potentials (active neurons) in KO mice compared to those in CR mice (Fig. 4A, B; CR: 36% (9 of
430 25 cells; N = 3) vs KO: 14% (5 of 35 cells; N = 4; χ^2 test, $\chi^2=3.84$, $P=0.05$). Whole-cell patch
431 clamp recordings revealed the decreased cell excitability in PVA neurons from the KO mice
432 was not due to significant differences in resting membrane potential between CR and KO cells
433 (CR: -55.5 ± 1.7 (n=35; N=9) and KO: -54.5 ± 1.7 (n=35; N=10), $p = 0.9$); however, input resistance
434 was significantly different between cells recorded from KO and CR mice (CR: 993.4 ± 52.9
435 (n=30; N=9) KO: 850.3 ± 40.7 (n=29; N = 9); $p = 0.04$). In addition, an increased action potential
436 threshold in KO compared to CR mice was observed (Fig. 4C; $t_{42} = 2.0$; $P < 0.05$). These results
437 suggest that reduced *Shox2* expression affects the firing properties of TCNs.

438 To investigate the spiking responses to depolarizing current injections, we recorded in
439 current clamp mode and injected 10-50 pA currents to evoke action potentials from resting
440 potential (-50 - 55 mV) and -70 mV. The number of action potentials fired in response to current
441 injection in neurons recorded from *Shox2* KO slices was significantly decreased compared to
442 that in neurons from CR slices at resting potentials (Fig. 4D; two-way repeat measures ANOVA:
443 main effect of current injection, $F_{4,148} = 59.9$, $P < 0.0001$; main effect of genotype, $F_{1,37} = 10.9$,
444 $P < 0.01$; interaction, $F_{4,148} = 4.06$, $P < 0.01$). Further investigation to determine effects on
445 bursting properties showed that the firing properties in response to depolarizing pulses from
446 -70 mV were not affected in the *Shox2* KO cells (Fig. 4E, Two way repeated measures ANOVA:
447 significant main effect of current injection $F_{4, 216} = 20.64$, $P < 0.0001$; but no significant main
448 effect of genotype CR vs KO, $F_{1, 54} = 4.2$, $P = 0.18$ or interaction $F_{4,216} = 0.49$; $P = 0.79$). These
449 results are consistent with the spontaneous firing results that suggest reduced *Shox2* affects
450 tonic TCN firing properties at depolarized membrane potentials.

451

452 **Shox2 is critical for HCN currents in the thalamus.**

453 Since HCN currents play a role in the firing properties of thalamocortical neurons^{74, 75},
454 and *Shox2* affects expression of *Hcn4* mRNA and protein, we investigated the effect of *Shox2*
455 KO on HCN current by sequential hyperpolarizations in voltage-clamp mode in the presence
456 of BaCl₂ to block inward rectifier K⁺ currents. The amplitude of HCN current was measured as
457 the difference between the end current of one-second hyperpolarization and the beginning
458 instantaneous current at -150mV hyperpolarization (Fig. 5A). The HCN current densities in
459 neurons from *Shox2* KO mice were significantly decreased compared to neurons from CR mice
460 ($t_{15}=3.1$; $P = 0.007$; Fig. 5B). Recordings were completed in current clamp to determine the
461 functional impact of reduced I_h , within the TCNs. Negative current injections from resting
462 potential (Fig. 5C; 10-90 pA in 10 pA steps) induced significantly smaller voltage sags in the KO
463 mice compared to CR mice (Fig. 5C,D; Two way ANOVA; main effect of current input $F_{(5, 55)} =$
464 24.5 ; $P < 0.0001$ and main effect of genotype $F_{(1, 11)} = 17.26$ but no interaction $F_{(5, 55)} = 0.4496$;
465 $P=0.8$). Upon release from the hyperpolarizing pulses, fewer KO cells (2/11) exhibited rebound
466 low threshold Ca²⁺ bursts compared to CR (7/10). These results suggest that *Shox2* KO reduced
467 I_h and physiologically impacts rebound firing of TCNs, that likely also involves T-type calcium
468 spikes. Significantly, the differences in sag were revealed in the presence of BaCl₂ and not in
469 control aCSF, which suggests that an inwardly rectifying K⁺ current may partially compensate
470 in the KO for the differences in I_h .

471 **Shox2 expression affects TCN synaptic activity.**

472 In order to determine the impact of *Shox2* KO on synaptic activity, excitatory
473 postsynaptic currents (EPSCs) were measured in cells from CR and KO mice. EPSC interevent
474 interval was significantly decreased in *Shox2* KO neurons compared to CR neurons (Fig. 6A-C;
475 $t_{50}=2.3$; $P = 0.03$), showing increased EPSC frequency in KO slices. Closer investigation revealed

476 instantaneous EPSC frequency was significantly increased in *Shox2* KO mice ($t_{50} = 3.0$; $P =$
477 0.004), suggesting increased EPSC burst frequency in slices from KO mice. Cumulative
478 frequency plots showed a significant shift toward increased instantaneous frequency
479 (Kolmogorov-Smirnov, $P < 0.0001$). There was no significant effect on mEPSC amplitude,
480 although a trend was observed ($t_{50} = 1.63$; $P = 0.1$). These results of increased instantaneous
481 frequency suggest increased burst glutamatergic input to PVA nucleus neurons in the *Shox2*
482 KO mice.

483 ***Shox2* KO induced thalamus-related behavioral deficits in adult mouse.**

484 The thalamus plays a critical role in sensory and motor information relay and processing,
485 sleep and arousal, learning and memory, as well as other cognitive functions. The
486 electrophysiological results indicated that *Shox2* KO impaired thalamic burst-related currents,
487 synaptic activity and intrinsic spiking properties. We hypothesized that *Shox2* is critical for
488 proper cognitive and somatosensory behavioral functions in adult mice. To study the specific
489 contribution of *Shox2* expression in the thalamus to behaviors, including anxiety, depression,
490 somatosensory information processing as well as learning and memory, two inducible KO
491 mouse strategies were employed. For the behavioral studies, we used the *Rosa26^{CreERT/+}*,
492 *Shox2^{-f}* mice line which is a tamoxifen-inducible global *Shox2* KO, and the *Gbx2^{CreERT/+}; Shox2⁻*
493 *^f* mice line which is also tamoxifen-inducible but restricts the KO of *Shox2* specifically in the
494 midline of the thalamus^{76, 77} and supplemental Fig. 2.

495 The total distance travelled in an open field test was measured to investigate the overall
496 activity and general anxiety levels. Distance travelled in the open field in the global *Shox2* KO
497 mice was not statistically significant compared to CR mice (Fig. 7A, $t_{26} = 1.48$; $p = 0.15$).
498 Interestingly, the global KO mice spent a significantly higher percentage of time in the center

499 of the open field compared to CR mice (Fig. 7B, $t_{26}=2.2$; $P=0.04$), which is indicative of lower
500 levels of anxiety in the KO mice ⁷⁸.

501 Because the open field test results suggested that global *Shox2* KO mice exhibited lower
502 anxiety, we investigated depressive-like behaviors using the tail suspension test and the forced
503 swim test in another cohort of animals ⁷⁹. In these tests, the time during which the animals
504 were actively struggling was measured as mobility time. We observed no significant difference
505 in mobility time between control and global KO mice in either test (Forced swim test, $t_{20}=0.39$,
506 $P=0.70$; Tail suspension, $t_{20}=0.85$, $P=0.40$; Supplemental Fig. 5A,B), suggesting *Shox2* KO did
507 not affect depressive-like behaviors.

508 To test the performance of the mice in general somatosensory function, the paw
509 sensation test was performed. Sticky tape was applied to the plantar surface of the right hind
510 paw of each mouse, and the latency to the mouse's first reaction to the tape was measured
511 ⁴⁹. The latency of KO mice to react to the tape was significantly longer than that of CR mice
512 (Fig. 7C; $t_{26}=2.38$, $P=0.03$). The results suggested that *Shox2* KO induced somatosensory
513 deficits in adult mice.

514 Given that anterior and medial thalamus are critical for learning and memory processes
515 ⁸⁰⁻⁸³, we tested a subset of the global *Shox2* KO mice in a novel object recognition test which
516 assesses learning and memory functions ^{84,85}. The test consisted of a familiarization trial and
517 a test trial. During the familiarization trial, we measured the time mice spent exploring 2
518 identical novel objects (see methods) in the open field environment. Animals of both
519 genotypes explored the 2 objects for similar amounts of time (Fig. 7E, Student's t-test, $t_{19}=1.7$,
520 $P=0.1$). Twenty-four hours later, in the memory test trial, the experiment was repeated but
521 one of the beakers was replaced with a new object (Fig. 7D). The percentage of time global
522 *Shox2* KO mice spent around the novel object was significantly decreased compared to that of

523 CR mice in the testing trial (Fig. 7F; $t_{19} = 2.1$, $P=0.05$). These results suggest an impairment of
524 learning and memory ability of global *Shox2* KO mice.

525 In order to determine whether the impairment in the object recognition test was
526 mediated by sensory or memory function, we also performed similar behavioral analysis in
527 the *Gbx2^{CreERT}; Shox2* KO mice (Fig. 7 G-K), where *Shox2* is reduced specifically in the medial
528 thalamus. The open field test was conducted to investigate the overall activity and general
529 anxiety level of CR and *Gbx2^{CreERT}; Shox^{fl/-}* KO mice. The total distance travelled by *Shox2* KO
530 mice was not significantly different compared to CR mice (Fig. 7G, $t_{21}=0.92$; $p = 0.37$). In
531 addition, unlike the global KO mice, the time spent in the center of the open field of *Gbx2^{CreERT};*
532 *Shox^{fl/-}* KO compared to CR mice was not significantly different (Figure 7H, $t_{21}=0.50$; $p = 0.62$).
533 We also tested the performance of these mice in general somatosensory function, with the
534 paw sensation test. The latency to react to the tape of KO mice was not significantly different
535 compared to CR mice (Fig. 7C; $t_{20}=0.4626$, $P=0.65$). The tape fell off the foot of one KO mouse,
536 therefore results from that animal were not used. The results suggested that *Shox2* KO in the
537 medial thalamus did not affect somatosensory function.

538 We also tested the *Gbx2^{CreERT}; Shox^{fl/-}* mice in the novel object recognition test as
539 described above. Animals of both genotypes explored the 2 objects for similar amounts of
540 time in the familiarization trial (Fig. 7J, Student's t-test, $t_{18}=1.64$; $P=0.11$). Twenty-four hours
541 later, in the memory test trial, the experiment was repeated but one of the beakers was
542 replaced with a new object (Fig. 7D). The percentage of time *Gbx2^{CreERT}; Shox^{fl/-}* mice spent
543 around the novel object was significantly decreased compared to that of CR mice in the testing
544 trial (Fig. 7F; $t_{18}=2.28$; $P=0.04$). These results suggest an impairment of memory formation in
545 the *Shox2* KO mice in the medial thalamus, consistent with studies that show the medial
546 thalamus is important for cognitive function.

547 Since the anterior and medial thalamus have also been implicated in fear memory
548 formation⁸⁶, cued and contextual fear memory was assessed. Neither contextual ($t_{21}=0.52$; p
549 = 0.61 nor cued fear memory ($t_{20}=0.14$; $p = 0.17$, freezing in one mouse was excluded as an
550 outlier) was affected in the *Gbx2*^{CreERT}; *Shox2*^{fl/-} KO mice (Supplemental Fig. 5C,D). This result is
551 supported by our observations made in td-Tomato animals that show sparse direct inputs to
552 the hippocampus and the amygdala (Fig. 2M-O). Together, these results suggest that the
553 groups of neurons expressing *Shox2* in medial thalamus support recognition memory but are
554 not implicated in fear memory formation or somatosensory information processing.

555

556 Discussion

557 This study demonstrates the importance of transcriptional activity of the homeobox
558 protein transcription factor, *Shox2*, in regulation of firing properties, synaptic connectivity, and
559 function of thalamocortical neurons in adult thalamus. This assertion is supported by our
560 investigations at genetic, electrophysiological and behavioral levels. Genetic analysis via RNA-
561 sequencing and Gene Ontology (GO) analysis revealed that *Shox2* modulates expression of
562 genes that encode for proteins directly associated with firing properties of TCNs, specifically
563 voltage-gated ion channels. Further investigation using quantitative PCR and Western blotting
564 showed that the mRNAs and proteins for several of these ion channels, namely HCN4 is down
565 regulated in the thalamus of the *Shox2* KO. Electrophysiological analysis showed that *Shox2*-
566 regulation of ion channels modulates the intrinsic firing properties in these neurons, reducing
567 neuronal excitability. In addition, the KO neurons received an increased frequency of EPSCs,
568 suggesting possible presynaptic mechanisms to compensate for decreased membrane
569 excitability to maintain TCN function. Finally, behavioral investigation revealed that global
570 *Shox2* KO mice were impaired in an object memory and somatosensory function test,

571 suggesting that *Shox2* is important to maintain normal function of thalamocortical neurons.
572 In order to discern the somatosensory deficit from the object memory function, we further
573 investigated mice with specific KO of *Shox2* in the medial thalamus KO (*Gbx2^{CreRrt}-Shox2*),
574 which maintained *Shox2* expression in the lateral thalamus, specifically the VB complex
575 important for somatosensory processing. These mice were impaired in the object recognition
576 task and not sensorimotor functions, suggesting that *Shox2* expression in the TCNs of the
577 medial thalamus is important for cognitive function. These studies are consistent with
578 previous results that show lesions to the anterior thalamic nuclei can disrupt object
579 recognition memory in animal models^{80, 82, 83, 87}.

580 Previous clinical studies demonstrated that proper thalamic function is critical for
581 memory formation and consolidation. In humans, damage to the thalamic nuclei, especially
582 medial and anterior nuclei, causes severe memory deficits known as diencephalic amnesia¹²⁻
583 ¹⁷. While the neural circuitry of the effects of *Shox2* expression on recognition memory are
584 unclear, perhaps these effects occur via effects on TCN connections to retrosplenial cortex as
585 suggested by the anatomical connectivity indicated in our study (Fig. 2 M-O). The retrosplenial
586 cortex has been linked to temporal order of recognition, also known as ‘what and when’
587 associations⁸⁸. Future studies are necessary to determine the specific projections and
588 functions of the firing properties of the TCNs involved in these functions.

589 Our investigations showed that *Shox2* KO affected tonic firing properties of TCNs. The
590 functions of the burst and tonic firing properties of thalamocortical neurons are still under
591 investigation. Tonic spike firing mode is thought to contribute to reliable information transfer
592 during perceptive states that conveys sensory information to cortex^{89, 90}. Burst firing mode
593 may allow lack of responsiveness to sensory input during sleep and unconsciousness such as
594 during an absence seizure⁹¹⁻⁹⁴. On the other hand, recent evidence suggests that thalamic

595 bursts can also occur during awake states and convey a high degree of information about
596 sensory stimuli to serve as a ‘wake-up call’ for cognitive attention⁹⁵⁻¹⁰⁰. Computational studies
597 suggest that the bursting behavior occurs in response to low-frequency stable inputs, while
598 single spikes occur in response to higher frequency more dynamic input^{101, 102}. Disruptions in
599 the transitions of firing patterns through effects on intrinsic currents in TCNs would disrupt
600 normal thalamic function and its contribution to information processing. Our present studies
601 from the thalamus, together with studies of *Shox2* function from the heart^{103, 104} and
602 excitatory interneurons in spinal cord^{34,36}, suggest that *Shox2* is important for maintenance of
603 tonic firing properties in TCNs.

604 Several lines of evidence indicate that these studies of the role of *Shox2* in pacemaker
605 function in mice are also applicable to humans. *Shox2* is a super-conserved gene with 99%
606 amino acid identity between human *SHOX2* and mouse *Shox2*. A recent study found that two
607 missense mutations within the human *SHOX2* gene are associated with early-onset atrial
608 fibrillation, likely caused by a defect in pacemaker activity^{105,106}. In addition, while mice do
609 not express the *Shox* gene, human *SHOX* and *SHOX2* have 79% similar amino acid identity, and
610 the same DNA-binding domains and putative phosphorylation sites. The functional
611 redundancy in the regulation of heart pacemaker cells’ differentiation between human *SHOX*
612 and mouse *Shox2* has been demonstrated in mouse models^{104, 107}. Therefore, investigation of
613 *Shox2* function in mouse can extend to evaluate the role of human *SHOX* and *SHOX2* in
614 humans. Turner syndrome (TS) is one of the most common sex chromosome abnormalities
615^{108, 109} and results from the complete or partial loss of the X chromosome. Most individuals
616 with TS have short stature, which is associated with the loss of the *SHOX* gene¹¹⁰⁻¹¹². These
617 individuals are at increased risk for neurodevelopmental issues, including learning disabilities,
618 visuo-spatial, social and executive function impairments¹¹³ and epilepsy¹¹⁴⁻¹¹⁸. Interestingly,

619 the smallest chromosomal deletion associated with the neurocognitive phenotype included
620 *SHOX*¹¹⁹, suggesting that loss of SHOX may play a role in cognitive impairments in humans.
621 While the mechanisms of the neurodevelopmental issues in these patients is unclear, our
622 current study indicates that altering expression of SHOX- or SHOX2-related genes may
623 contribute to thalamic dysfunctions and some of these neurodevelopmental impairments.

624 Further studies are necessary to determine the specific contribution of *Shox2*-expressing
625 neurons to thalamocortical circuitry, and the role *Shox2* may play beyond regulation of firing
626 properties. In addition, future studies will investigate whether *Shox2* plays a critical role during
627 thalamus development and differentiation, the contribution of these *Shox2*-regulated
628 currents to overall thalamocortical neuron function, and the mechanisms by which *Shox2*
629 regulates their expression.

630

631 **Figure Legends**

632

633 **Figure 1. *Shox2* is expressed in NeuN+ neurons in the thalamus and not in GFAP+ astrocytes.**
634 Coronal brain sections through the thalamus of *Shox2*^{Cre/+}, Rosa26LacZ mice were co-stained
635 with NeuN (green) and β -gal (red). Three typical thalamic regions are shown, including
636 anterior paraventricular thalamus (PVA) (A), dorsal lateral geniculate nucleus (dLGN) (B), and
637 ventrobasal nucleus (VB) (C). Slices were co-stained for NeuN and the reporter for *Shox2*, β -
638 gal. *Shox2* is expressed in NeuN+ neurons (red, merged). Right panels are magnifications of
639 the boxed regions respectively, showing cells that co-express *Shox2* and NeuN. D-F show the
640 co-expression of astrocyte marker GFAP (green) and β -gal (red), in three thalamic regions: PVA
641 (D), dLGN (E) and VB (F). Right panels are magnifications of the boxed regions. The arrowheads
642 show the GFAP+ glia, and the white arrows show *Shox2*-expressing cells as indicated by β -gal.
643 No cells co-expressed GFAP and *Shox2*. RT: reticular thalamus. AV: anteroventral nucleus of
644 the thalamus; AD: anterodorsal nucleus of the thalamus. HP: hippocampus.

645

646 **Figure 2. *Shox2* is expressed in glutamatergic thalamocortical neurons but not parvalbumin+
647 interneurons.** Coronal sections through the thalamus were co-stained with parvalbumin
648 (green, A, B) and β -gal (red, A, C). Boxes in Figure A are magnified in D. (habenula), E.
649 Ventrobasal (VB) and reticular nucleus (RT), and F. dorsal lateral geniculate nucleus (dLGN). G.
650 Panels G-I show *Shox2* expression in coronal slices of rostral to caudal thalamus (G:
651 Paraventricular nucleus of the thalamus (PVA) relative to Bregma, approx. -1.1; H: lateral
652 geniculate nucleus (LGN) -2.0; I: Medial geniculate nucleus (MGN) -2.9). M-O: Coronal
653 sections from rostral (M) to caudal (O) from the Ai27D-*Shox2Cre* in which the presence of
654 tdTomato indicates *Shox2*-expressing neurons. *Shox2* is expressed in neurons throughout the

655 thalamus and projections to the cortex, strongly targeting layer IV barrel cortex (white arrows)
656 and layer VI.

657

658

659 **Figure 3. *Shox2* expression affects gene expression and ion channel protein levels.** RNA-
660 sequencing and analysis were performed as described in methods. **A.** Heatmap, made by
661 pheatmap, saturated at 1, displays 367 DEGs (adjusted p value <0.1) in the medial thalamus
662 between control (CR) and *Gbx2^{CreErt}, Shox2* KO mice. **B.** Gene ontology (GO) enrichment
663 analysis of DEGs. All terms with an FDR (analyzed by DAVID functional annotation tool) less
664 than 0.1 are listed. **C-E.** RT-qPCR results show that *Shox2* KO significantly reduced mRNA level
665 of *Cacna1g*. (**C**), *Hcn2* (**D**) and *Hcn4* (**E**). **F-H.** *Shox2* KO decreased the protein expression levels
666 of Ca_v3.1 (**F**, ~120kD), HCN2 (**G**, ~150kD), and HCN4 (**H**, >250kD) (**, p < 0.01; *, p<0.05, #,
667 p<0.1). The bands around ~55-60kD are recognized by the β-tubulin antibody.

668

669 **Figure 4. *Shox2* KO decreases excitability of TCNs in anterior paraventricular thalamus (PVA).**

670 **A.** Example traces of attached-cell recordings of active cells showing spontaneous action
671 potentials (left) and inactive cells with no action potentials (right). **B.** Bar graph representing
672 the ratio of active and inactive cells recorded in PVA from KO and CR mice. This ratio is
673 significantly smaller in KO than in CR mice (*, p<0.05; n = 9 of 25 CR cells (N = 3) and 5 of 25
674 KO cells (N = 4). **C.** Whole-cell patch clamp recordings showed that action potential threshold
675 was significantly increased in *Shox2* KO cells compared to CR cells (KO: n= 16; N= 6; CR: n =23,
676 N= 9; p =0.04). **D.** Example traces of firing patterns triggered by the injection of ramp current
677 (10-50 pA) from near membrane potential (-55 mV) in cells recorded from CR – left, black)
678 and KO mice (right, gray). Right –graph showing reduced spike number in KO cells compared
679 to CR cells at all membrane potentials when depolarized from -55 mV. **E.** Example traces of
680 spike firing triggered by the injection of ramp current (10-50 pA) from -70 mV in cells recorded
681 from CR – left, black) and KO mice (right, gray). Right –graph showing no significant change in
682 spike number in KO cells compared to CR cells at all membrane potentials when depolarized
683 from -70 mV. (*, p < 0.05, **, p < 0.01, ***, p <0.001).

684

685 **Figure 5. *Shox2* KO decreased HCN current in anterior PVT of neurons.** **A.** An example of HCN
686 current elicited by hyperpolarizing cell membrane from -50mV to -100mV and -150mV. HCN
687 current is defined as the current difference between the current at the end of 1s
688 hyperpolarization and the current peak at the beginning of hyperpolarization as shown in the
689 figure. **B.** Scatter plot showing that *Shox2* KO (n = 9; N = 3) decreased HCN current density in
690 anterior PVT of neurons (**, P<0.01) compared to CR neurons (n = 8; N = 2). **C.** Example
691 current clamp recordings demonstrating inhibitory pulses and sag in CR and KO mice. **D.**
692 Current voltage plot showing sag amplitude measured in response to negative current
693 injection (90-10 pA). (**, P < 0.01; n = 7; N= 2; KO n = 6, N = 3)

694

695 **Figure 6. Cells from *Shox2* KO mice receive increased frequency of EPSCs.** **A.** Example of
696 EPSCs and EPSPs (below) recorded from KO (upper) and CR (lower) mice. **B.** Quantification of
697 interevent interval, *Shox2* KO cells showed reduced interevent interval (*, P < 0.05; KO: n =
698 23; N= 9; CR: n = 29, N = 8). **C.** Quantification of instantaneous frequency, *Shox2* KO cells
699 showed increased instantaneous frequency (**, P < 0.01). **D.** Cumulative frequency of
700 instantaneous frequency shows a significant shift toward higher frequencies in KO slices

701 (****, $P < 0.0001$; Kolmogorov Smirnov test). E. No significant effect of *Shox2* KO was
702 observed in on EPSC amplitude.

703

704 **Figure 7. *Shox2* inducible KO caused comprehensive thalamus-related behavior deficits. A.**
705 Results from open field analysis. The total distances travelled by *Rosa^{CreErt}, Shox2* KO and CR
706 mice in 5-minute open field test were similar. **B.** *Rosa^{CreErt}, Shox2* KO mice spent a higher
707 percentage of time in the center of open field than CR mice (*, $P < 0.05$). **C.** Mice with a ~ 1 cm²
708 sticky tape on the left hind paw were placed in home cage and the latency for the mice to
709 first react to the tape was measured. *Shox2* KO mice had a longer latency to first react to the
710 tapes than CR mice ($P < 0.01$). **D-E.** The results of discrimination index showed that *Shox2* KO
711 impaired mice ability in recognizing novel object in testing trial (*, $P = 0.02$), while there was
712 no object preference difference between CR and KO mice in familiarization trial ($P = 0.33$). **F.**
713 The total distance travelled by *Gbx2^{CreErt}, Shox2* KO mice in 5-minute open field test was
714 significantly decreased compared to that by CR mice. **G.** *Gbx2^{CreErt}, Shox2* KO mice spent a
715 similar percentage of time in the center of compared to CR mice. **H.** *Gbx2^{CreErt}, Shox2* KO mice
716 were not significantly different from CR in the sticky tape test. **I-J.** Object recognition task in
717 *Gbx2^{CreErt}, Shox2* KO mice. The results of discrimination index showed that *Gbx2^{CreErt}, Shox2* KO
718 impaired mice ability in recognizing novel object in testing trial ($p < 0.05$) (K), while there was
719 no object preference different between CR and KO mice in familiarization trial (J).

720

721

722 Supplemental Figures

723 **Supplemental Figure 1.** Schematic diagrams of breeding schemes used to produce
724 *Rosa26^{CreERT/CreERT}, Shox2^{f/-}* and *Gbx2^{CreErt/CreErt}, Shox^{f/-}* mice.

725 **Supplemental Figure 2. Characterization of *Gbx2* expression and *Gbx2*-induced *Shox2* KO in**
726 **thalamus. A.** GFP staining (red color) represented the expression pattern of *Gbx2* in P25
727 mouse brain, showing *Gbx2* only expressed in the midline of the thalamus (arrow shows PVT
728 in midline thalamus) but not lateral thalamus. Blue: DAPI. **B.** qPCR results demonstrating
729 significant knockdown of *Shox2* mRNA in medial thalamus of *Gbx2^{CreErt/CreErt}, Shox^{f/-}* mice
730 compared to CR mice ($t_6 = 3.9$, $P = 0.008$), but no effect on *Shox2* mRNA expression in the
731 lateral thalamus compared to CR animals (**, $p < 0.01$).

732

733 **Supplemental Figure 3. *Shox2* expression is restricted to thalamus in adult and diencephalon**
734 **throughout development.** Brain sections demonstrating X-gal staining (or *Shox2* expression)
735 results from PND25 (**A1-A8**) and PND56 *Shox2^{LacZ/+}* (**B1-B4**) and PND56 male *Shox2^{cre/+},*
736 *Rosa26^{LacZ/+}* mouse (**C1-C4**). X-gal staining was observed in anterior thalamus nuclei (ATN),
737 anterior paraventricular nucleus (PVA), ventrobasal thalamus (VB), dorsal lateral geniculate
738 nucleus (dLGN) and medial geniculate nucleus (MGN) but was not observed in the cortex (CX),
739 striatum (STR), hippocampus (HP), amygdala (Ag) or hypothalamus (HT). During development,
740 *Shox2* did express in in habenula (HB), and some areas of the midbrain including superior
741 colliculus (SC) and inferior colliculus (IC), but this expression is reduced in adults. Scale bar: 2
742 mm.

743

744 **Supplemental Figure 4. Strong GFAP immunoreactivity in the hippocampus, but a lack of**
745 **GFAP+ staining in the thalamus.** Coronal brain section showing strong GFAP+ staining in the
746 hippocampus, but a dearth of GFAP staining in the thalamus.

747

748 **Supplemental Figure 5. Behavioral analysis of Shox2 KO mice.** Mobility results measured
749 from CR and *RosaCre;Shox2* KO mice. Forced swim test (A) and tail suspension test (B). No
750 significant differences in struggling time between CR and KO mice were observed. C,D.
751 Freezing behavior measured in cued and contextual fear conditioning in *Gbx2Cre; Shox2KO*
752 mice. No significant differences in freezing behavior to the context or cue were observed.

753

754 **Acknowledgements:** Funding NIH grants R21NS101482 to LAS and R01 HL136326 to YPC.

755 **Authorship statement:** DY and MM conceived experimental design, performed experiments,
756 and wrote the manuscript. YS, XH, IF, CN, EM, SR contributed data. CS, WY (posthumous)
757 contributed to early planning stages. YPC provided animals and reagents and LAS contributed
758 to overall design and wrote manuscript.

759

760

761

762 **References :**

763

- 764 1. Bal, T. & McCormick, D.A. What stops synchronized thalamocortical oscillations? *Neuron* **17**, 297-308
765 (1996).
- 766 2. Kim, J.H., Kim, J.B., Seo, W.K., Suh, S.I. & Koh, S.B. Volumetric and shape analysis of thalamus in
767 idiopathic generalized epilepsy. *J Neurol* **260**, 1846-1854 (2013).
- 768 3. Williams, D. The thalamus and epilepsy. *Brain : a journal of neurology* **88**, 539-556 (1965).
- 769 4. Mory, S.B. *et al.* Structural abnormalities of the thalamus in juvenile myoclonic epilepsy. *Epilepsy &*
770 *behavior : E&B* **21**, 407-411 (2011).
- 771 5. Nair, A., Treiber, J.M., Shukla, D.K., Shih, P. & Muller, R.A. Impaired thalamocortical connectivity in autism
772 spectrum disorder: a study of functional and anatomical connectivity. *Brain : a journal of neurology* **136**,
773 1942-1955 (2013).
- 774 6. Tsatsanis, K.D. *et al.* Reduced thalamic volume in high-functioning individuals with autism. *Biol*
775 *Psychiatry* **53**, 121-129 (2003).
- 776 7. Muller, R.A. *et al.* Underconnected, but how? A survey of functional connectivity MRI studies in autism
777 spectrum disorders. *Cerebral cortex* **21**, 2233-2243 (2011).
- 778 8. Andreasen, N.C. The role of the thalamus in schizophrenia. *Can J Psychiatry* **42**, 27-33 (1997).
- 779 9. Brickman, A.M. *et al.* Thalamus size and outcome in schizophrenia. *Schizophr Res* **71**, 473-484 (2004).
- 780 10. Pinault, D. Dysfunctional thalamus-related networks in schizophrenia. *Schizophr Bull* **37**, 238-243 (2011).
- 781 11. Woodward, N.D., Karbasforoushan, H. & Heckers, S. Thalamocortical dysconnectivity in schizophrenia.
782 *Am J Psychiatry* **169**, 1092-1099 (2012).
- 783 12. Warren, J.D., Thompson, P.D. & Thompson, P.D. Diencephalic amnesia and apraxia after left thalamic
784 infarction. *J Neurol Neurosurg Psychiatry* **68**, 248 (2000).

- 785 13. Van der Werf, Y.D., Jolles, J., Witter, M.P. & Uylings, H.B. Contributions of thalamic nuclei to declarative
786 memory functioning. *Cortex* **39**, 1047-1062 (2003).
- 787 14. Thielen, J.W., Takashima, A., Rutters, F., Tendolkar, I. & Fernandez, G. Transient relay function of midline
788 thalamic nuclei during long-term memory consolidation in humans. *Learning & memory* **22**, 527-531
789 (2015).
- 790 15. Graff-Radford, N.R., Tranel, D., Van Hoesen, G.W. & Brandt, J.P. Diencephalic amnesia. *Brain : a journal*
791 *of neurology* **113 (Pt 1)**, 1-25 (1990).
- 792 16. Garden, D.L. *et al.* Anterior thalamic lesions stop synaptic plasticity in retrosplenial cortex slices:
793 expanding the pathology of diencephalic amnesia. *Brain : a journal of neurology* **132**, 1847-1857 (2009).
- 794 17. Dzieciol, A.M. *et al.* Hippocampal and diencephalic pathology in developmental amnesia. *Cortex* **86**, 33-
795 44 (2017).
- 796 18. Llinas, R. & Jahnsen, H. Electrophysiology of mammalian thalamic neurones in vitro. *Nature* **297**, 406-
797 408 (1982).
- 798 19. Jahnsen, H. & Llinas, R. Ionic basis for the electro-responsiveness and oscillatory properties of guinea-
799 pig thalamic neurones in vitro. *The Journal of physiology* **349**, 227-247 (1984).
- 800 20. Deschenes, M., Paradis, M., Roy, J.P. & Steriade, M. Electrophysiology of neurons of lateral thalamic
801 nuclei in cat: resting properties and burst discharges. *Journal of neurophysiology* **51**, 1196-1219 (1984).
- 802 21. McCormick, D.A. & Bal, T. Sleep and arousal: thalamocortical mechanisms. *Annual review of*
803 *neuroscience* **20**, 185-215 (1997).
- 804 22. Clement-Jones, M. *et al.* The short stature homeobox gene SHOX is involved in skeletal abnormalities in
805 Turner syndrome. *Human molecular genetics* **9**, 695-702 (2000).
- 806 23. De Baere, E., Speleman, F., Van Roy, N., De Paepe, A. & Messiaen, L. Assignment of SHOX2 (alias OG12X
807 and SHOT) to human chromosome bands 3q25-->q26.1 by in situ hybridization. *Cytogenetics and cell*
808 *genetics* **82**, 228-229 (1998).
- 809 24. Sun, C., Zhang, T., Liu, C., Gu, S. & Chen, Y. Generation of Shox2-Cre allele for tissue specific manipulation
810 of genes in the developing heart, palate, and limb. *Genesis* **51**, 515-522 (2013).
- 811 25. Greisas, A. & Zlochiver, S. Modulation of cardiac pacemaker inter beat intervals by sinoatrial fibroblasts
812 -a numerical study. *Conf Proc IEEE Eng Med Biol Soc* **2016**, 165-168 (2016).
- 813 26. Cribbs, L. T-type calcium channel expression and function in the diseased heart. *Channels (Austin)* **4**,
814 447-452 (2010).
- 815 27. Ludwig, A. *et al.* Absence epilepsy and sinus dysrhythmia in mice lacking the pacemaker channel HCN2.
816 *The EMBO journal* **22**, 216-224 (2003).
- 817 28. Sun, C. *et al.* The short stature homeobox 2 (Shox2)-bone morphogenetic protein (BMP) pathway
818 regulates dorsal mesenchymal protrusion development and its temporary function as a pacemaker
819 during cardiogenesis. *The Journal of biological chemistry* **290**, 2007-2023 (2015).
- 820 29. Ye, W. *et al.* A common Shox2-Nkx2-5 antagonistic mechanism primes the pacemaker cell fate in the
821 pulmonary vein myocardium and sinoatrial node. *Development* **142**, 2521-2532 (2015).
- 822 30. Ionta, V. *et al.* SHOX2 overexpression favors differentiation of embryonic stem cells into cardiac
823 pacemaker cells, improving biological pacing ability. *Stem cell reports* **4**, 129-142 (2015).
- 824 31. Wang, J. *et al.* Pitx2 prevents susceptibility to atrial arrhythmias by inhibiting left-sided pacemaker
825 specification. *Proceedings of the National Academy of Sciences of the United States of America* **107**,
826 9753-9758 (2010).
- 827 32. Rosin, J.M., Kurrasch, D.M. & Cobb, J. Shox2 is required for the proper development of the facial motor
828 nucleus and the establishment of the facial nerves. *BMC neuroscience* **16**, 39 (2015).
- 829 33. Rosin, J.M. *et al.* Mice lacking the transcription factor SHOX2 display impaired cerebellar development
830 and deficits in motor coordination. *Developmental biology* **399**, 54-67 (2015).
- 831 34. Dougherty, K.J. *et al.* Locomotor rhythm generation linked to the output of spinal shox2 excitatory

- 832 interneurons. *Neuron* **80**, 920-933 (2013).
- 833 35. Abdo, H. *et al.* Dependence on the transcription factor Shox2 for specification of sensory neurons
834 conveying discriminative touch. *The European journal of neuroscience* **34**, 1529-1541 (2011).
- 835 36. Ha, N.T. & Dougherty, K.J. Spinal Shox2 interneuron interconnectivity related to function and
836 development. *Elife* **7** (2018).
- 837 37. Soriano, P. Generalized lacZ expression with the ROSA26 Cre reporter strain. *Nat Genet* **21**, 70-71 (1999).
- 838 38. Patro, R., Duggal, G., Love, M.I., Irizarry, R.A. & Kingsford, C. Salmon provides fast and bias-aware
839 quantification of transcript expression. *Nat Methods* **14**, 417-419 (2017).
- 840 39. Love, M.I., Huber, W. & Anders, S. Moderated estimation of fold change and dispersion for RNA-seq data
841 with DESeq2. *Genome Biol* **15**, 550 (2014).
- 842 40. Huang da, W., Sherman, B.T. & Lempicki, R.A. Systematic and integrative analysis of large gene lists using
843 DAVID bioinformatics resources. *Nat Protoc* **4**, 44-57 (2009).
- 844 41. Huang da, W., Sherman, B.T. & Lempicki, R.A. Bioinformatics enrichment tools: paths toward the
845 comprehensive functional analysis of large gene lists. *Nucleic acids research* **37**, 1-13 (2009).
- 846 42. Valente, V. *et al.* Selection of suitable housekeeping genes for expression analysis in glioblastoma using
847 quantitative RT-PCR. *BMC molecular biology* **10**, 17 (2009).
- 848 43. Li, B. *et al.* Identification of optimal reference genes for RT-qPCR in the rat hypothalamus and intestine
849 for the study of obesity. *Int J Obes (Lond)* **38**, 192-197 (2014).
- 850 44. Puil, E., Gimbarzevsky, B. & Miura, R.M. Quantification of membrane properties of trigeminal root
851 ganglion neurons in guinea pigs. *Journal of neurophysiology* **55**, 995-1016 (1986).
- 852 45. Zhang, C., Bosch, M.A., Rick, E.A., Kelly, M.J. & Ronnekleiv, O.K. 17Beta-estradiol regulation of T-type
853 calcium channels in gonadotropin-releasing hormone neurons. *The Journal of neuroscience : the official
854 journal of the Society for Neuroscience* **29**, 10552-10562 (2009).
- 855 46. Bhattacharjee, A., Whitehurst, R.M., Jr., Zhang, M., Wang, L. & Li, M. T-type calcium channels facilitate
856 insulin secretion by enhancing general excitability in the insulin-secreting beta-cell line, INS-1.
857 *Endocrinology* **138**, 3735-3740 (1997).
- 858 47. Lee, J.H., Gomora, J.C., Cribbs, L.L. & Perez-Reyes, E. Nickel block of three cloned T-type calcium channels:
859 low concentrations selectively block alpha1H. *Biophysical journal* **77**, 3034-3042 (1999).
- 860 48. Antunes, M. & Biala, G. The novel object recognition memory: neurobiology, test procedure, and its
861 modifications. *Cogn Process* **13**, 93-110 (2012).
- 862 49. Arakawa, H. *et al.* Thalamic NMDA receptor function is necessary for patterning of the thalamocortical
863 somatosensory map and for sensorimotor behaviors. *The Journal of neuroscience : the official journal
864 of the Society for Neuroscience* **34**, 12001-12014 (2014).
- 865 50. Can, A. *et al.* The mouse forced swim test. *J Vis Exp*, e3638 (2012).
- 866 51. Gusel'nikova, V.V. & Korzhevskiy, D.E. NeuN As a Neuronal Nuclear Antigen and Neuron Differentiation
867 Marker. *Acta Naturae* **7**, 42-47 (2015).
- 868 52. Herculano-Houzel, S. & Lent, R. Isotropic fractionator: a simple, rapid method for the quantification of
869 total cell and neuron numbers in the brain. *The Journal of neuroscience : the official journal of the
870 Society for Neuroscience* **25**, 2518-2521 (2005).
- 871 53. Eng, L.F. Glial fibrillary acidic protein (GFAP): the major protein of glial intermediate filaments in
872 differentiated astrocytes. *J Neuroimmunol* **8**, 203-214 (1985).
- 873 54. Yang, Z. & Wang, K.K. Glial fibrillary acidic protein: from intermediate filament assembly and gliosis to
874 neurobiomarker. *Trends in neurosciences* **38**, 364-374 (2015).
- 875 55. Arcelli, P., Frassoni, C., Regondi, M.C., De Biasi, S. & Spreafico, R. GABAergic neurons in mammalian
876 thalamus: a marker of thalamic complexity? *Brain research bulletin* **42**, 27-37 (1997).
- 877 56. Song, I. *et al.* Role of the alpha1G T-type calcium channel in spontaneous absence seizures in mutant
878 mice. *The Journal of neuroscience : the official journal of the Society for Neuroscience* **24**, 5249-5257

- 879 (2004).
- 880 57. Kim, D. *et al.* Lack of the burst firing of thalamocortical relay neurons and resistance to absence seizures
881 in mice lacking alpha(1G) T-type Ca(2+) channels. *Neuron* **31**, 35-45 (2001).
- 882 58. Zhang, Y., Vilaythong, A.P., Yoshor, D. & Noebels, J.L. Elevated thalamic low-voltage-activated currents
883 precede the onset of absence epilepsy in the SNAP25-deficient mouse mutant coloboma. *The Journal*
884 *of neuroscience : the official journal of the Society for Neuroscience* **24**, 5239-5248 (2004).
- 885 59. Talley, E.M. *et al.* Differential distribution of three members of a gene family encoding low voltage-
886 activated (T-type) calcium channels. *The Journal of neuroscience : the official journal of the Society for*
887 *Neuroscience* **19**, 1895-1911 (1999).
- 888 60. Kim, D. *et al.* Lack of the burst firing of thalamocortical relay neurons and resistance to absence seizures
889 in mice lacking alpha(1G) T-type Ca(2+) channels, *Neuron* **31**, 35-45 (2001).
- 890 61. Anderson, M.P. *et al.* Thalamic Cav3.1 T-type Ca²⁺ channel plays a crucial role in stabilizing sleep.
891 *Proceedings of the National Academy of Sciences of the United States of America* **102**, 1743-1748 (2005).
- 892 62. Moosmang, S., Biel, M., Hofmann, F. & Ludwig, A. Differential distribution of four hyperpolarization-
893 activated cation channels in mouse brain. *Biological chemistry* **380**, 975-980 (1999).
- 894 63. Llinas, R.R. & Steriade, M. Bursting of thalamic neurons and states of vigilance. *Journal of*
895 *neurophysiology* **95**, 3297-3308 (2006).
- 896 64. Puil, E., Meiri, H. & Yarom, Y. Resonant behavior and frequency preferences of thalamic neurons. *Journal*
897 *of neurophysiology* **71**, 575-582 (1994).
- 898 65. Hutcheon, B., Miura, R.M., Yarom, Y. & Puil, E. Low-threshold calcium current and resonance in thalamic
899 neurons: a model of frequency preference. *Journal of neurophysiology* **71**, 583-594 (1994).
- 900 66. Hutcheon, B. & Yarom, Y. Resonance, oscillation and the intrinsic frequency preferences of neurons.
901 *Trends in neurosciences* **23**, 216-222 (2000).
- 902 67. Xue, W.N. *et al.* SK- and h-current contribute to the generation of theta-like resonance of rat substantia
903 nigra pars compacta dopaminergic neurons at hyperpolarized membrane potentials. *Brain Struct Funct*
904 **217**, 379-394 (2012).
- 905 68. Hu, H., Vervaeke, K. & Storm, J.F. Two forms of electrical resonance at theta frequencies, generated by
906 M-current, h-current and persistent Na⁺ current in rat hippocampal pyramidal cells. *The Journal of*
907 *physiology* **545**, 783-805 (2002).
- 908 69. Williams, S.R., Toth, T.I., Turner, J.P., Hughes, S.W. & Crunelli, V. The 'window' component of the low
909 threshold Ca²⁺ current produces input signal amplification and bistability in cat and rat thalamocortical
910 neurones. *The Journal of physiology* **505 (Pt 3)**, 689-705 (1997).
- 911 70. Hughes, S.W., Cope, D.W., Toth, T.I., Williams, S.R. & Crunelli, V. All thalamocortical neurones possess a
912 T-type Ca²⁺ 'window' current that enables the expression of bistability-mediated activities. *The Journal*
913 *of physiology* **517 (Pt 3)**, 805-815 (1999).
- 914 71. Crunelli, V., Toth, T.I., Cope, D.W., Blethyn, K. & Hughes, S.W. The 'window' T-type calcium current in
915 brain dynamics of different behavioural states. *The Journal of physiology* **562**, 121-129 (2005).
- 916 72. Crunelli, V., Cope, D.W. & Hughes, S.W. Thalamic T-type Ca²⁺ channels and NREM sleep. *Cell calcium* **40**,
917 175-190 (2006).
- 918 73. Dreyfus, F.M. *et al.* Selective T-type calcium channel block in thalamic neurons reveals channel
919 redundancy and physiological impact of I(T)window. *The Journal of neuroscience : the official journal of*
920 *the Society for Neuroscience* **30**, 99-109 (2010).
- 921 74. Zobeiri, M. *et al.* Modulation of thalamocortical oscillations by TRIP8b, an auxiliary subunit for HCN
922 channels. *Brain Struct Funct* (2017).
- 923 75. Zobeiri, M. *et al.* The Hyperpolarization-Activated HCN4 Channel is Important for Proper Maintenance
924 of Oscillatory Activity in the Thalamocortical System. *Cerebral cortex* (2019).
- 925 76. Mallika, C., Guo, Q. & Li, J.Y. Gbx2 is essential for maintaining thalamic neuron identity and repressing

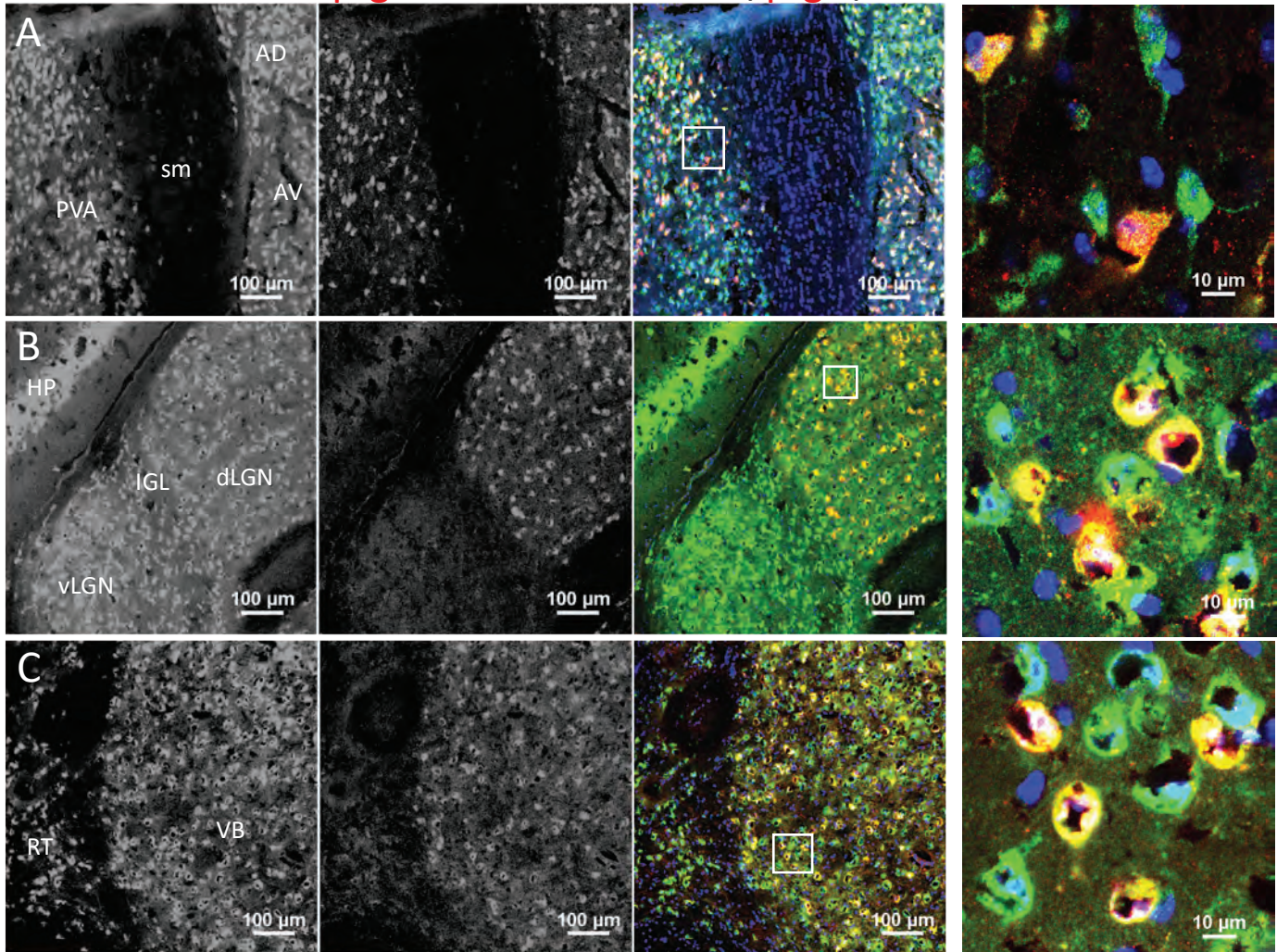
- 926 habenular characters in the developing thalamus. *Developmental biology* **407**, 26-39 (2015).
- 927 77. Chen, L., Guo, Q. & Li, J.Y. Transcription factor Gbx2 acts cell-nonautonomously to regulate the formation
928 of lineage-restriction boundaries of the thalamus. *Development* **136**, 1317-1326 (2009).
- 929 78. Seibenhener, M.L. & Wooten, M.C. Use of the Open Field Maze to measure locomotor and anxiety-like
930 behavior in mice. *J Vis Exp*, e52434 (2015).
- 931 79. Castagne, V., Moser, P., Roux, S. & Porsolt, R.D. Rodent models of depression: forced swim and tail
932 suspension behavioral despair tests in rats and mice. *Curr Protoc Neurosci* **Chapter 8**, Unit 8 10A (2011).
- 933 80. Jankowski, M.M. *et al.* The anterior thalamus provides a subcortical circuit supporting memory and
934 spatial navigation. *Frontiers in systems neuroscience* **7**, 45 (2013).
- 935 81. Aggleton, J.P. & Sahgal, A. The contribution of the anterior thalamic nuclei to anterograde amnesia.
936 *Neuropsychologia* **31**, 1001-1019 (1993).
- 937 82. Aggleton, J.P. & Mishkin, M. Memory impairments following restricted medial thalamic lesions in
938 monkeys. *Experimental brain research* **52**, 199-209 (1983).
- 939 83. Aggleton, J.P., Dumont, J.R. & Warburton, E.C. Unraveling the contributions of the diencephalon to
940 recognition memory: a review. *Learning & memory* **18**, 384-400 (2011).
- 941 84. Vogel-Ciernia, A. & Wood, M.A. Examining object location and object recognition memory in mice. *Curr*
942 *Protoc Neurosci* **69**, 8 31 31-17 (2014).
- 943 85. Murai, T., Okuda, S., Tanaka, T. & Ohta, H. Characteristics of object location memory in mice: Behavioral
944 and pharmacological studies. *Physiology & behavior* **90**, 116-124 (2007).
- 945 86. Padilla-Coreano, N., Do-Monte, F.H. & Quirk, G.J. A time-dependent role of midline thalamic nuclei in
946 the retrieval of fear memory. *Neuropharmacology* **62**, 457-463 (2012).
- 947 87. Dumont, J.R. & Aggleton, J.P. Dissociation of recognition and recency memory judgments after anterior
948 thalamic nuclei lesions in rats. *Behavioral neuroscience* **127**, 415-431 (2013).
- 949 88. Powell, A.L. *et al.* The retrosplenial cortex and object recency memory in the rat. *The European journal*
950 *of neuroscience* **45**, 1451-1464 (2017).
- 951 89. Elijah, D.H., Samengo, I. & Montemurro, M.A. Thalamic neuron models encode stimulus information by
952 burst-size modulation. *Front Comput Neurosci* **9**, 113 (2015).
- 953 90. Sherman, S.M. Dual response modes in lateral geniculate neurons: mechanisms and functions. *Vis*
954 *Neurosci* **13**, 205-213 (1996).
- 955 91. McCormick, D.A. & Pape, H.C. Properties of a hyperpolarization-activated cation current and its role in
956 rhythmic oscillation in thalamic relay neurones. *The Journal of physiology* **431**, 291-318 (1990).
- 957 92. McCormick, D.A. & Feuser, H.R. Functional implications of burst firing and single spike activity in lateral
958 geniculate relay neurons. *Neuroscience* **39**, 103-113 (1990).
- 959 93. Jeanmonod, D., Magnin, M. & Morel, A. Low-threshold calcium spike bursts in the human thalamus.
960 Common physiopathology for sensory, motor and limbic positive symptoms. *Brain : a journal of*
961 *neurology* **119 (Pt 2)**, 363-375 (1996).
- 962 94. Guillery, R.W. & Sherman, S.M. Thalamic relay functions and their role in corticocortical communication:
963 generalizations from the visual system. *Neuron* **33**, 163-175 (2002).
- 964 95. Sherman, S.M. & Guillery, R.W. The role of the thalamus in the flow of information to the cortex. *Philos*
965 *Trans R Soc Lond B Biol Sci* **357**, 1695-1708 (2002).
- 966 96. Sherman, S.M. & Guillery, R.W. Functional organization of thalamocortical relays. *Journal of*
967 *neurophysiology* **76**, 1367-1395 (1996).
- 968 97. Sherman, S.M. A wake-up call from the thalamus. *Nature neuroscience* **4**, 344-346 (2001).
- 969 98. Reinagel, P., Godwin, D., Sherman, S.M. & Koch, C. Encoding of visual information by LGN bursts. *Journal*
970 *of neurophysiology* **81**, 2558-2569 (1999).
- 971 99. Marlinski, V. & Beloozerova, I.N. Burst firing of neurons in the thalamic reticular nucleus during
972 locomotion. *Journal of neurophysiology* **112**, 181-192 (2014).

- 973 100. Guido, W., Lu, S.M. & Sherman, S.M. Relative contributions of burst and tonic responses to the receptive
974 field properties of lateral geniculate neurons in the cat. *Journal of neurophysiology* **68**, 2199-2211
975 (1992).
- 976 101. Zeldenrust, F., Wadman, W.J. & Englitz, B. Neural Coding With Bursts-Current State and Future
977 Perspectives. *Front Comput Neurosci* **12**, 48 (2018).
- 978 102. Zeldenrust, F., Chameau, P. & Wadman, W.J. Spike and burst coding in thalamocortical relay cells. *PLoS*
979 *Comput Biol* **14**, e1005960 (2018).
- 980 103. Liu, H. *et al.* The role of Shox2 in SAN development and function. *Pediatric cardiology* **33**, 882-889 (2012).
- 981 104. Liu, H. *et al.* Functional redundancy between human SHOX and mouse Shox2 genes in the regulation of
982 sinoatrial node formation and pacemaking function. *The Journal of biological chemistry* **286**, 17029-
983 17038 (2011).
- 984 105. Li, N. *et al.* A SHOX2 loss-of-function mutation underlying familial atrial fibrillation. *Int J Med Sci* **15**,
985 1564-1572 (2018).
- 986 106. Hoffmann, S. *et al.* Coding and non-coding variants in the SHOX2 gene in patients with early-onset atrial
987 fibrillation. *Basic research in cardiology* **111**, 36 (2016).
- 988 107. Liu, H. *et al.* Phosphorylation of Shox2 is required for its function to control sinoatrial node formation.
989 *Journal of the American Heart Association* **3**, e000796 (2014).
- 990 108. Nielsen, J. & Wohler, M. Sex chromosome abnormalities found among 34,910 newborn children:
991 results from a 13-year incidence study in Arhus, Denmark. *Birth Defects Orig Artic Ser* **26**, 209-223 (1990).
- 992 109. Jacobs, P. *et al.* Turner syndrome: a cytogenetic and molecular study. *Ann Hum Genet* **61**, 471-483 (1997).
- 993 110. Oliveira, C.S. & Alves, C. The role of the SHOX gene in the pathophysiology of Turner syndrome.
994 *Endocrinologia y nutricion : organo de la Sociedad Espanola de Endocrinologia y Nutricion* **58**, 433-442
995 (2011).
- 996 111. Joseph, M. *et al.* Xp pseudoautosomal gene haploinsufficiency and linear growth deficiency in three
997 girls with chromosome Xp22;Yq11 translocation. *Journal of medical genetics* **33**, 906-911 (1996).
- 998 112. Blaschke, R.J. *et al.* SHOT, a SHOX-related homeobox gene, is implicated in craniofacial, brain, heart, and
999 limb development. *Proceedings of the National Academy of Sciences of the United States of America* **95**,
1000 2406-2411 (1998).
- 1001 113. Mauger, C. *et al.* Executive Functions in Children and Adolescents with Turner Syndrome: A Systematic
1002 Review and Meta-Analysis. *Neuropsychol Rev* **28**, 188-215 (2018).
- 1003 114. Zhao, H. & Lian, Y.J. Epilepsy associated with Turner syndrome. *Neurol India* **63**, 631-633 (2015).
- 1004 115. Saad, K. *et al.* Turner syndrome: review of clinical, neuropsychiatric, and EEG status: an experience of
1005 tertiary center. *Acta Neurol Belg* **114**, 1-9 (2014).
- 1006 116. Puusepp, H., Zordania, R., Paal, M., Bartsch, O. & Ounap, K. Girl with partial Turner syndrome and
1007 absence epilepsy. *Pediatr Neurol* **38**, 289-292 (2008).
- 1008 117. Magara, S. *et al.* Rub epilepsy in an infant with Turner syndrome. *Brain Dev* **37**, 725-728 (2015).
- 1009 118. Jhang, K.M., Chang, T.M., Chen, M. & Liu, C.S. Generalized epilepsy in a patient with mosaic Turner
1010 syndrome: a case report. *J Med Case Rep* **8**, 109 (2014).
- 1011 119. Knickmeyer, R.C. & Davenport, M. Turner syndrome and sexual differentiation of the brain: implications
1012 for understanding male-biased neurodevelopmental disorders. *J Neurodev Disord* **3**, 293-306 (2011).
- 1013

NeuN

β -gal

NeuN/ β -gal/DAPI



GFAP

β -gal

DAPI/GFAP/ β -gal

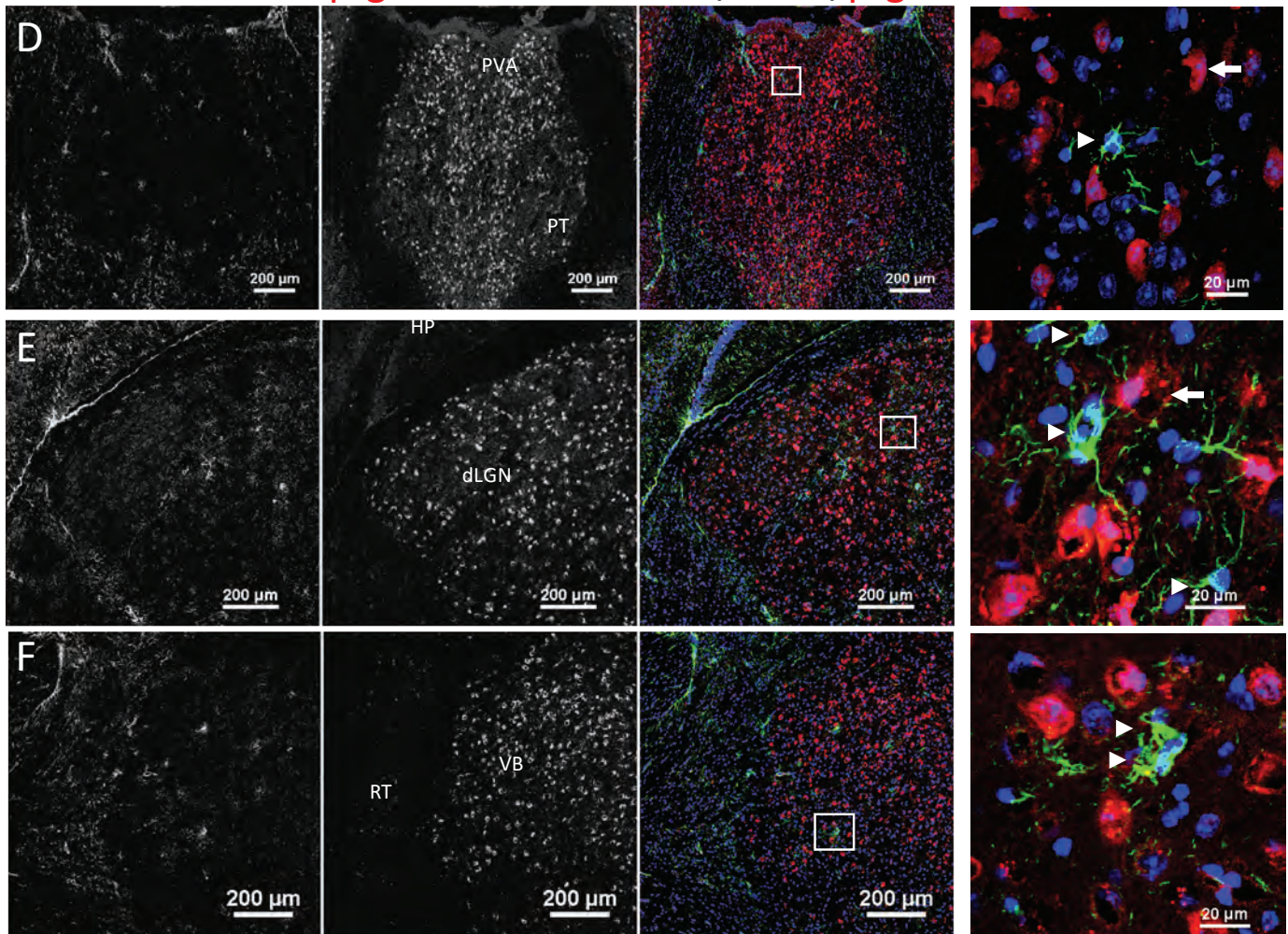
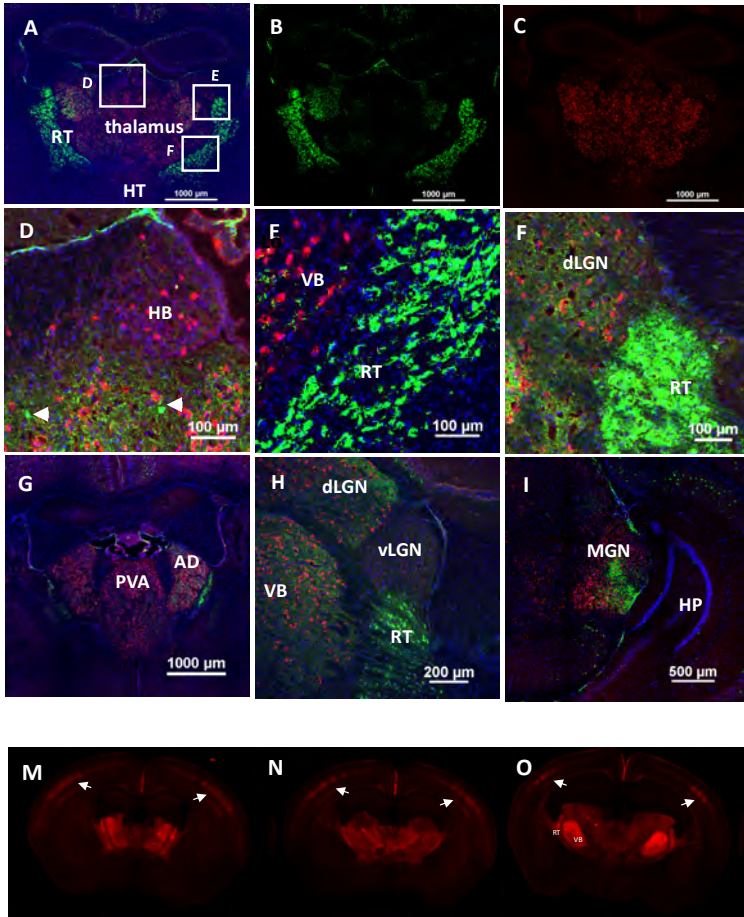


Figure 2. Yu et. al.

DAPI/PV/ β -gal



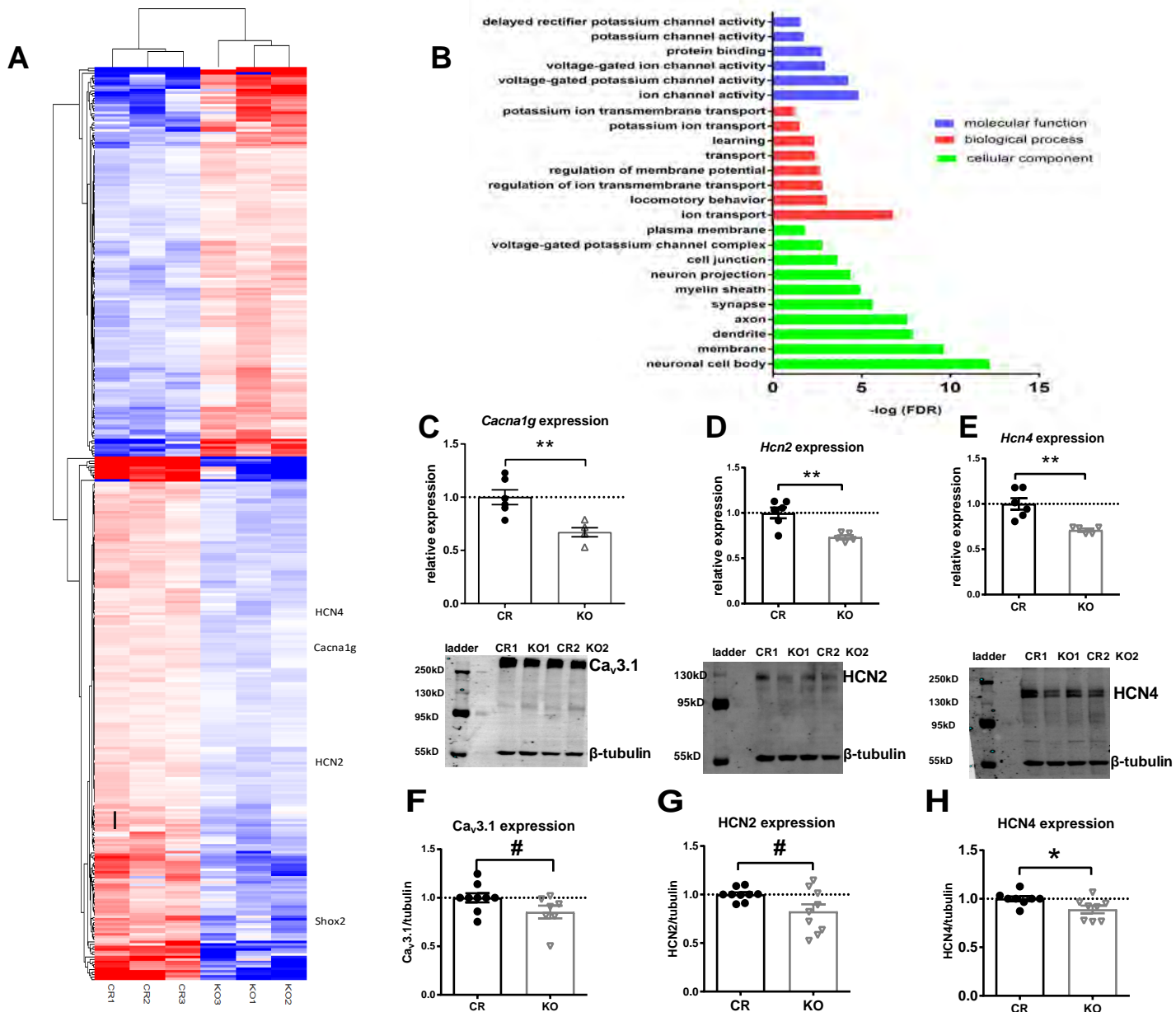


Figure 3. Yu et al

